An Absolute Microscopic Calibration of a Dual-Phase Xenon TPC

A Measurement of the Mean Electronic Excitation Energy of Liquid Xenon

Laura Baudis, Patricia Sanchez-Lucas, Kevin Thieme

University of Zurich

xenoscope.org

arXiv:2109.07151

Applications of Liquid Xenon Detectors

Direct Dark Matter Detection

- WIMPs, ALPs, …
- Dual-phase Time Projection Chambers (TPCs): XENONnT, LUX-ZEPLIN, PandaX, DARWIN
- Single-phase: XMASS

Cold head of Xenoscope
L. Baudis et al. JINST 16 (2021) P08052

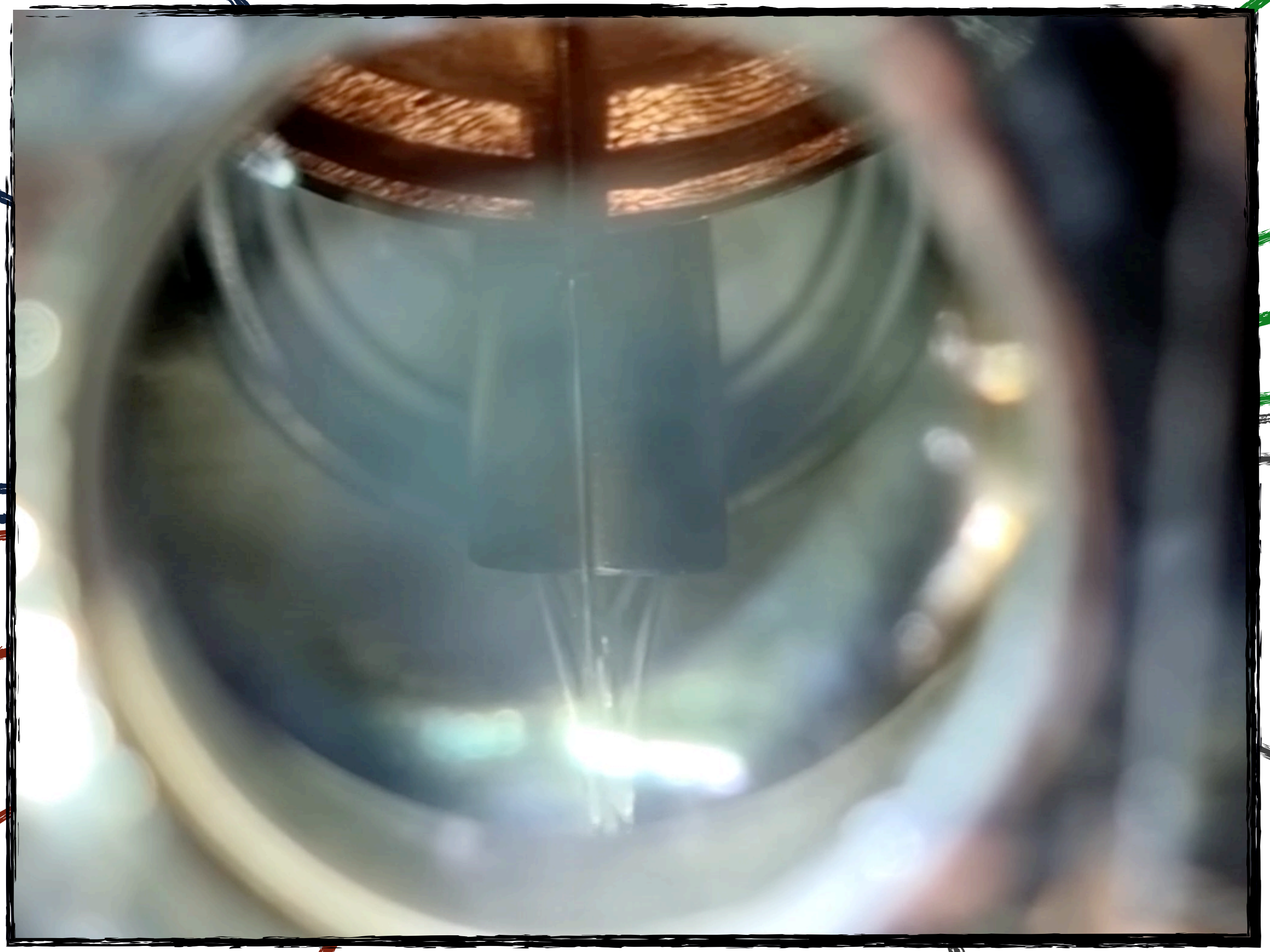

Rare Decays

- $\pi \to \mu\nu\gamma$: RAPID
- $\mu \to e\gamma$: MEG
- ^{124}Xe ECEC: XENON1T

Neutrino Physics

- $0\nu\beta\beta$ decay: EXO-200, nEXO, current generation TPCs and DARWIN
- Low-energy solar neutrinos, supernova neutrinos, CEνNS: current generation TPCs and DARWIN

E. Aprile and T. Doke
Rev. Mod. Phys. 82 (2010), 2053

Other

Medical Imaging: SPECT, PET (e.g. XEMIS prototypes, NIM A 912 (2018) 329)

Gamma-Ray Astrophysics: TPC as Compton telescope on balloon (LXeGRIT prototype, New Astron. Rev. 48 (2004) 257)

Calorimetry in HEP: Prototypes (NIM A 234 (1990) 439, NIM A 451 (2000) 427)

Particle Interaction in Liquid Xenon

Energy deposition -> Scintillation (direct + recombination) + Ionisation + Heat

Excitation

Dual-Phase Xenon Time Projection Chamber

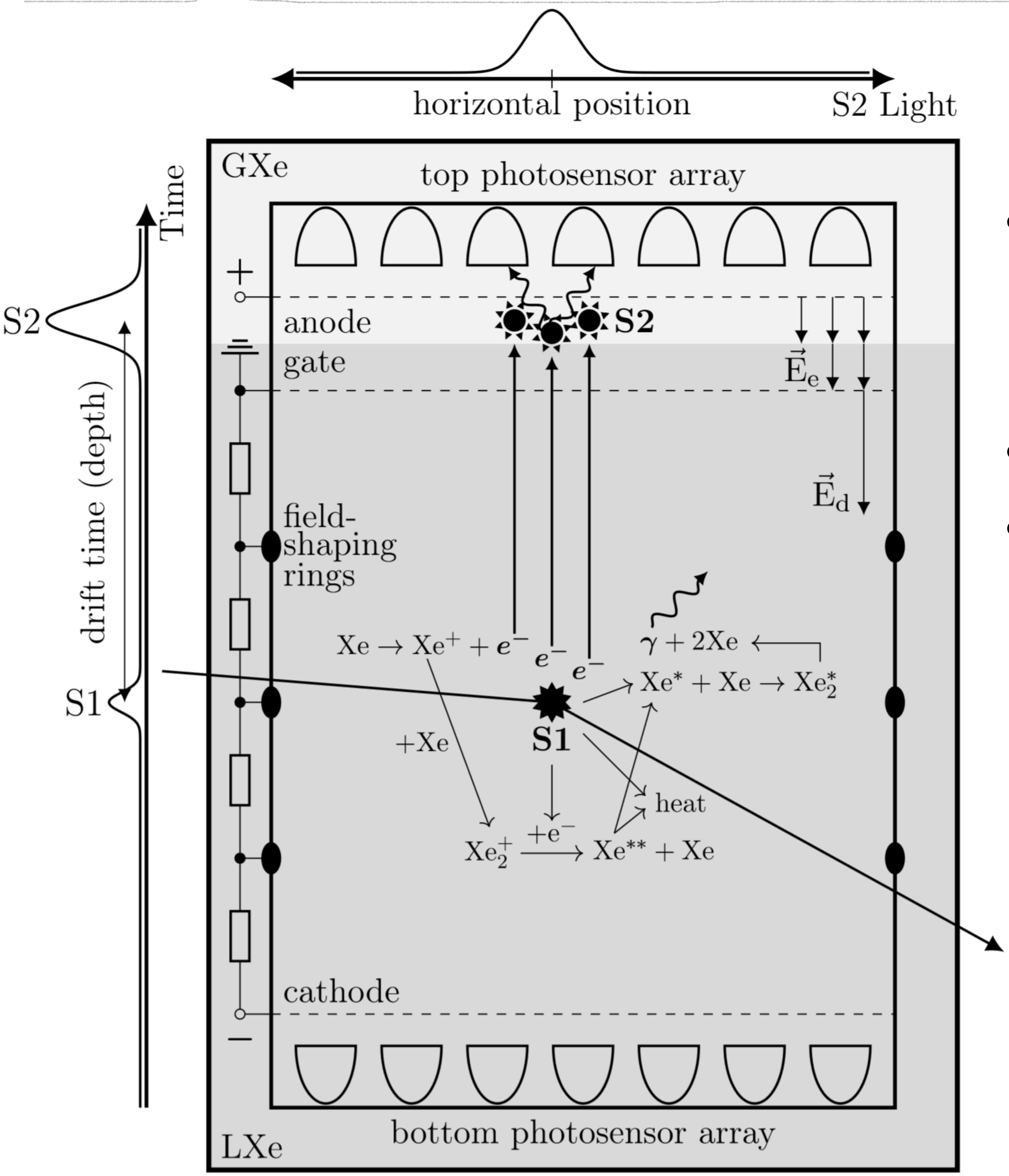

- Detection of prompt scintillation (S1) and delayed ionisation signal (S2)
- Heat not accessible with TPCs
- 3D position reconstruction

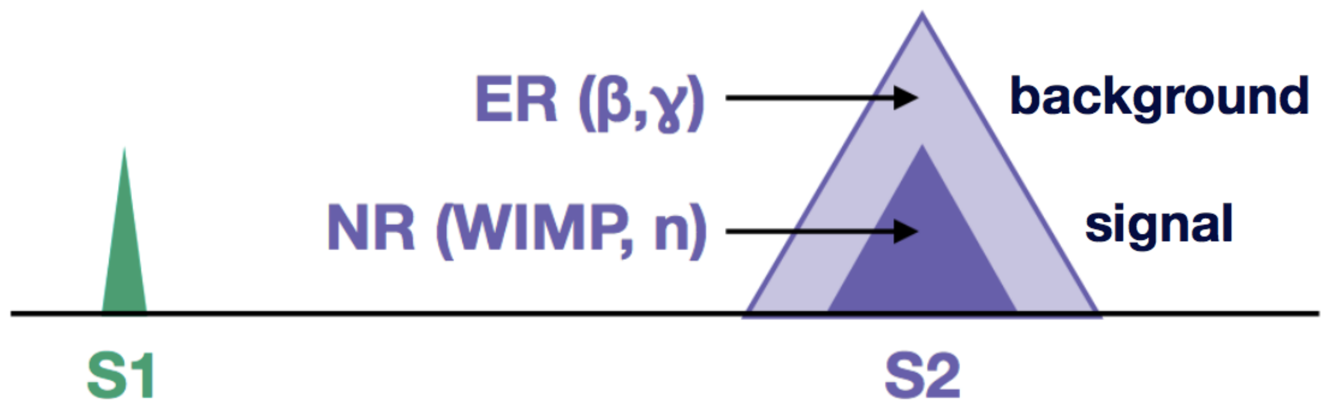

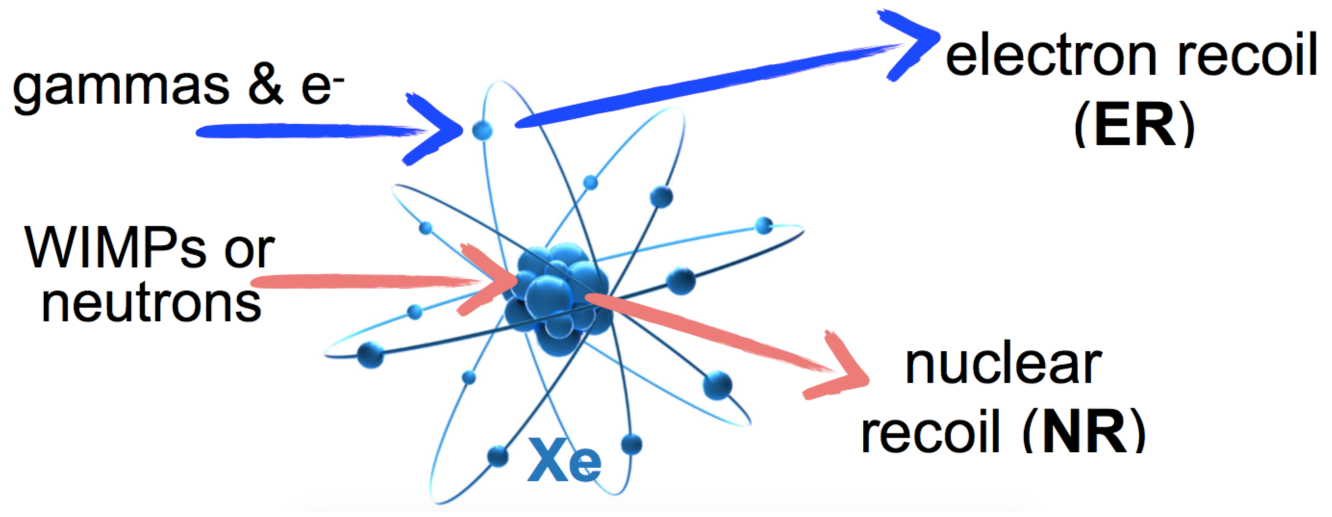

- ER/NR discrimination based on S1/S2 ratio

Mean Electronic Excitation Energy of LXe

- Sum of excitation quanta proportional to energy deposition, scintillation and ionisation signals are anti-correlated
- Model LXe excitation with *work function* W – average energy to produce a quantum (e^-, γ) in an (ER) interaction of energy E

$$E = (n_\gamma + n_{e^-})W$$

#ɣ from direct excitation and recombined e^-

#e^- extracted

- Mean value, we do not subdivide into W for scintillation and W for ionisation
- W defines the recombination-independent microscopic absolute energy scale of LXe detectors

  <-> Unlike relative calibration w.r.t. energy lines from calibration sources

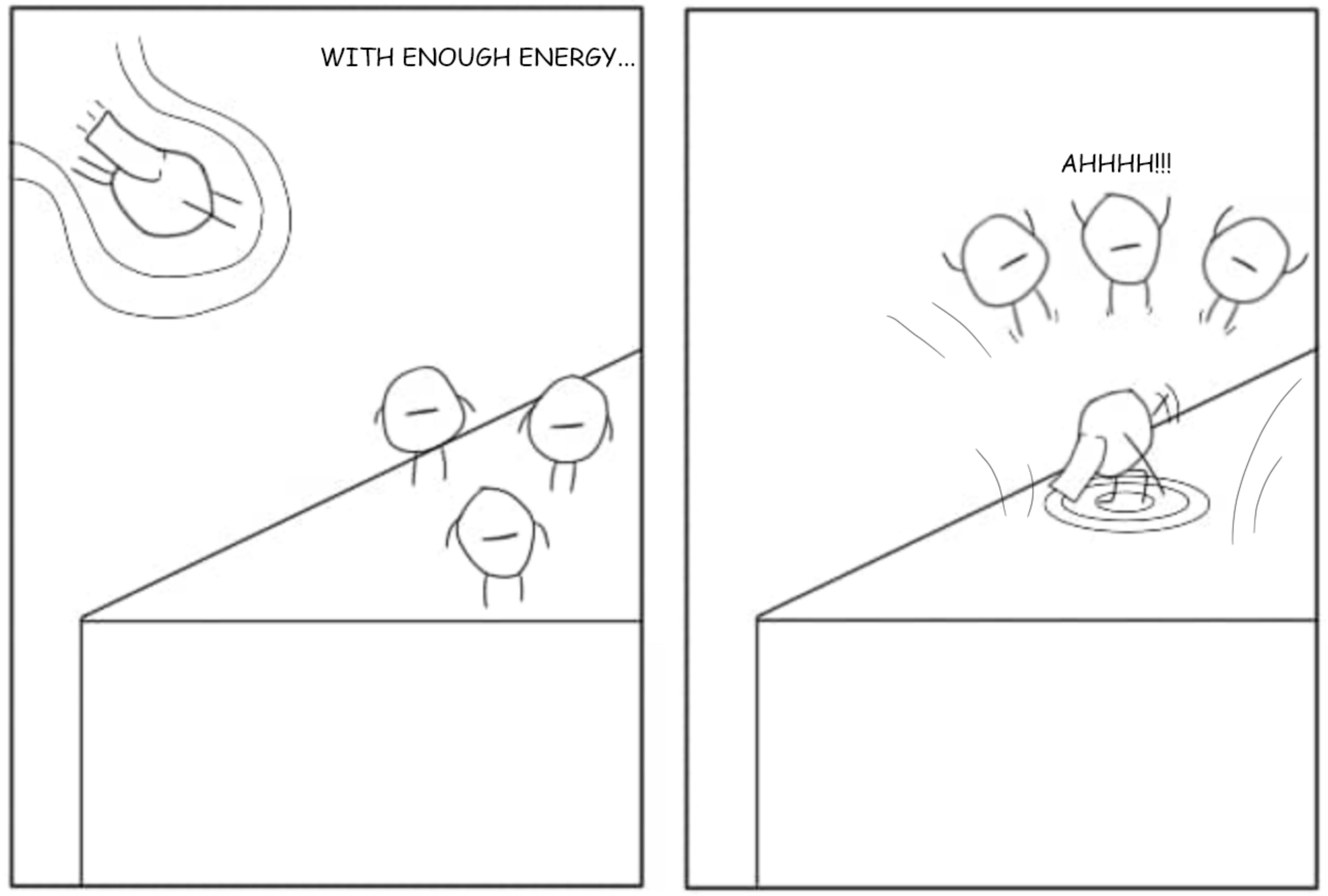

https://i.redd.it/1mo8ju8i3my51.png

Assumption:
e^--ion-recombination yields 1 photon

Literature Values of W

- Widely used value measured by E. Dahl [1]:

$$\mathbf{W = (13.7 \pm 0.2)\ eV}$$

  ➡ With a ^{57}Co source at ~100 keV

  ➡ Small TPC with PMTs operated in **single** and **dual** phase mode

  ➡ Absolute charge yield calibration with an amplifier on the anode

  ➡ Consistent with former measurements

- 2 years ago EXO-200 reported on a measurement with $\mathcal{O}$ (1 MeV) gamma sources [2]:

$$\mathbf{W = (11.5 \pm 0.1\,(stat.) \pm 0.5\,(syst.))\ eV}$$

  ➡ **Single** phase detector with wire charge and LAAPD light readout

  ➡ Absolute charge calibration of amplifier on readout plane

W (eV)	W_i (eV)	Particle type	Year	Ref.
–	15.6 ± 0.3	e^- (976 keV)	1975	[31]
–	13.6 ± 0.2	γ (662 keV)	1979	[32]
14.7 ± 1.5	–	e^- (976 keV)	1990	[36,37]
–	9.76 ± 0.70	e^- (0.02–3 GeV)	1992	[33]
13.8 ± 0.9	–	e^- (976 keV)	2002	[16]
13.46 ± 0.29	–	γ (122 keV)	2007	[13]
13.7 ± 0.2	–	γ (122 keV, 136 keV)	2009	[12]
14.0	–	γ (164 keV)	2010	[35]
13.7 ± 0.4	–	Compilation	2011	[9]
–	16.5 ± 0.8	γ (122 keV)	2011	[18]
–	14.30 ± 0.14	Compilation	2014	[20]

Table taken from [2], references can be found therein

[1] C. E. Dahl, PhD Thesis, Princeton University (2009)
[2] EXO-200 Collaboration, Phys. Rev. C 101, 065501 (2020)

What we have in our lab in Zurich…

Xurich II TPC with SiPMs

- Small dual-phase TPC designed to study low-energy interactions
- 2 × 2 S13371 VUV-4 MPPCs from Hamamatsu on ×10 pre-amplifier board in the top array – 16 channels
- 2-inch R6041-06 PMT from Hamamatsu at the bottom
- 10 kV/cm extraction field (5.4 kV/cm in LXe)
- Up to 1 kV/cm drift field

L.. Baudis et al., EPJ C 80, 477 (2020)

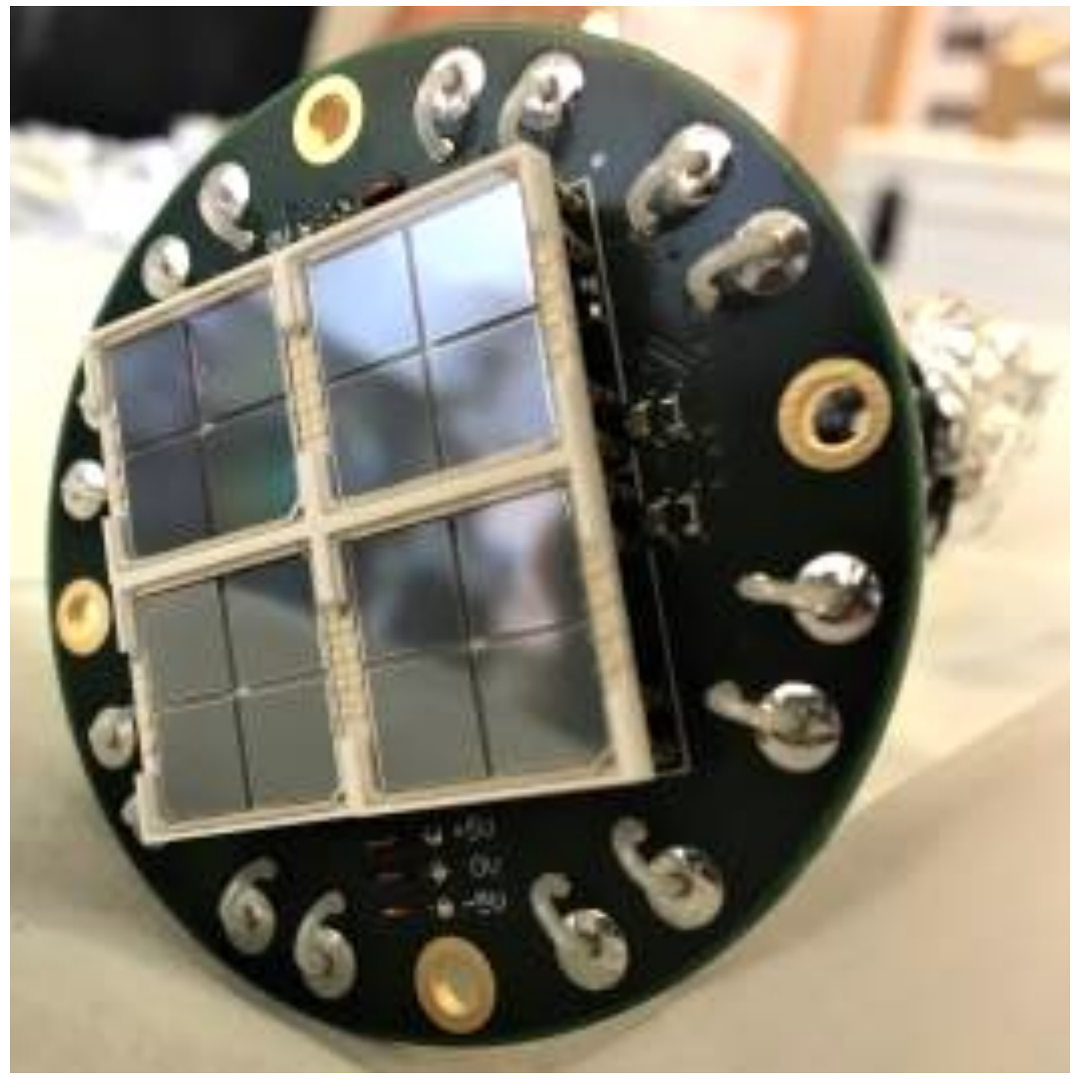

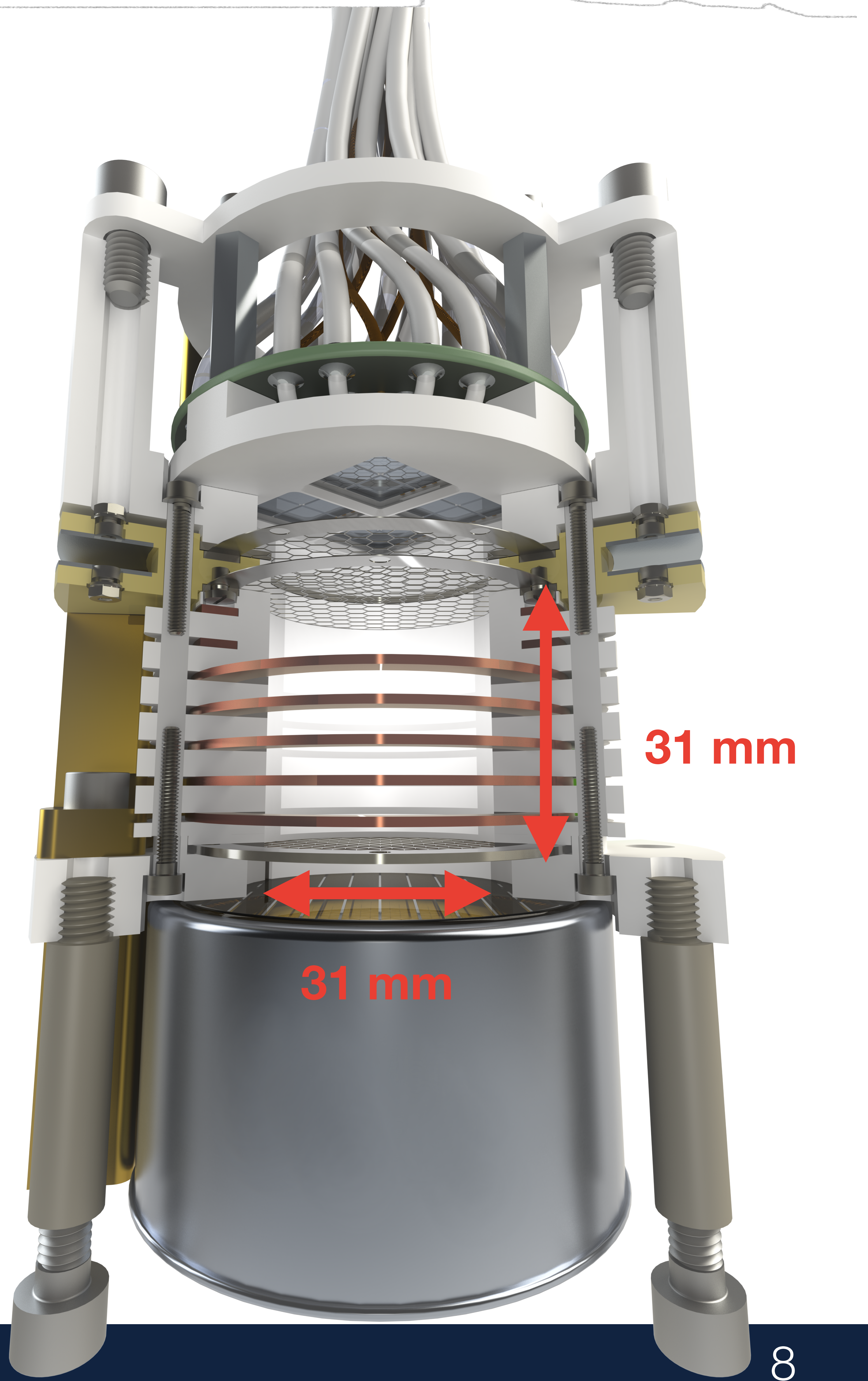

SiPM Performance

- Gain: (3.12 ± 0.01) x 10^6 (< 6 % variation among channels)
- Horizontal position reconstruction resolution: ~1.5 mm
- Error-weighted mean DC rate: (8.05 ± 0.03) Hz/mm^2 at 190 K, 51.5 V
- Crosstalk probability: (2.2 ± 0.1) %

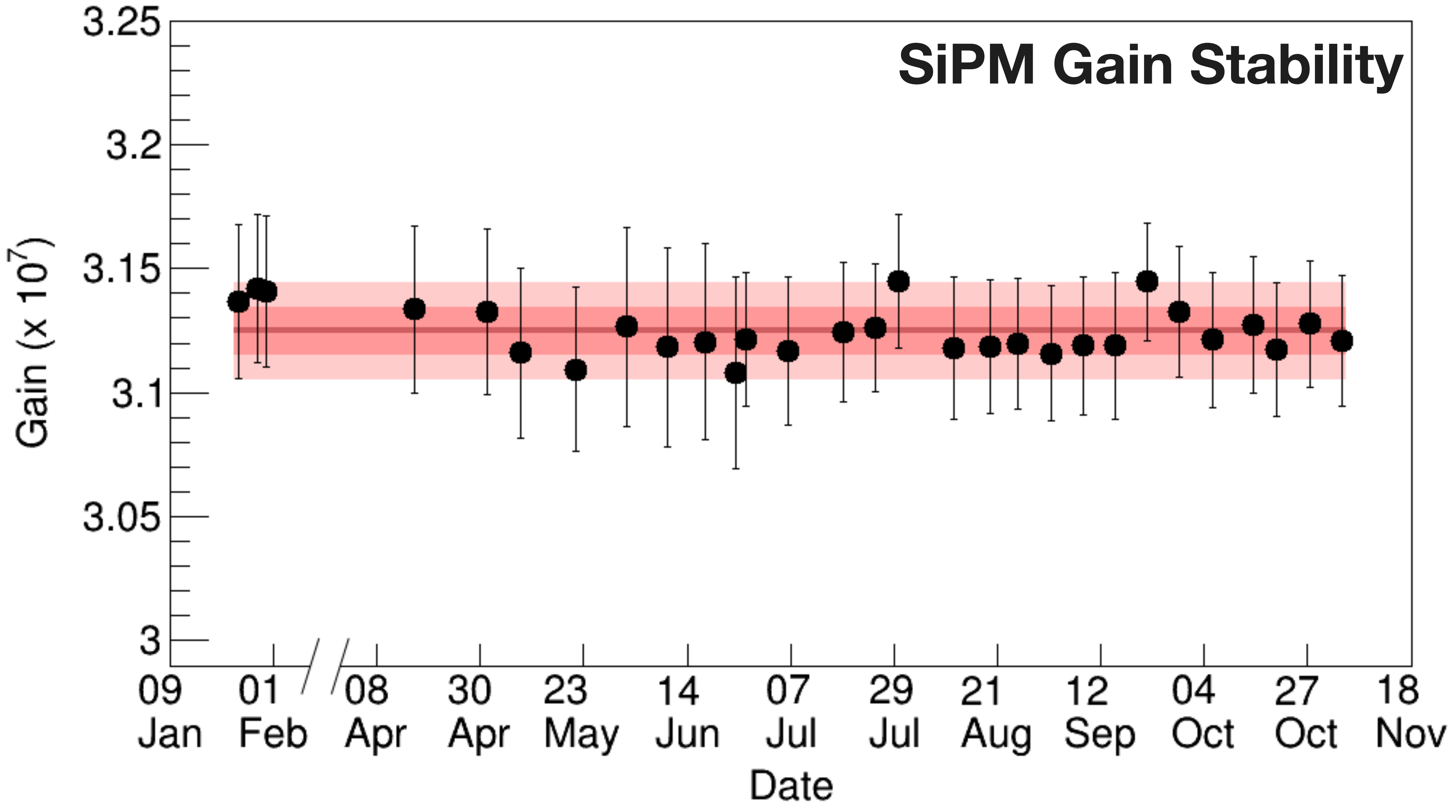

EPJ C 80, 477 (2020)

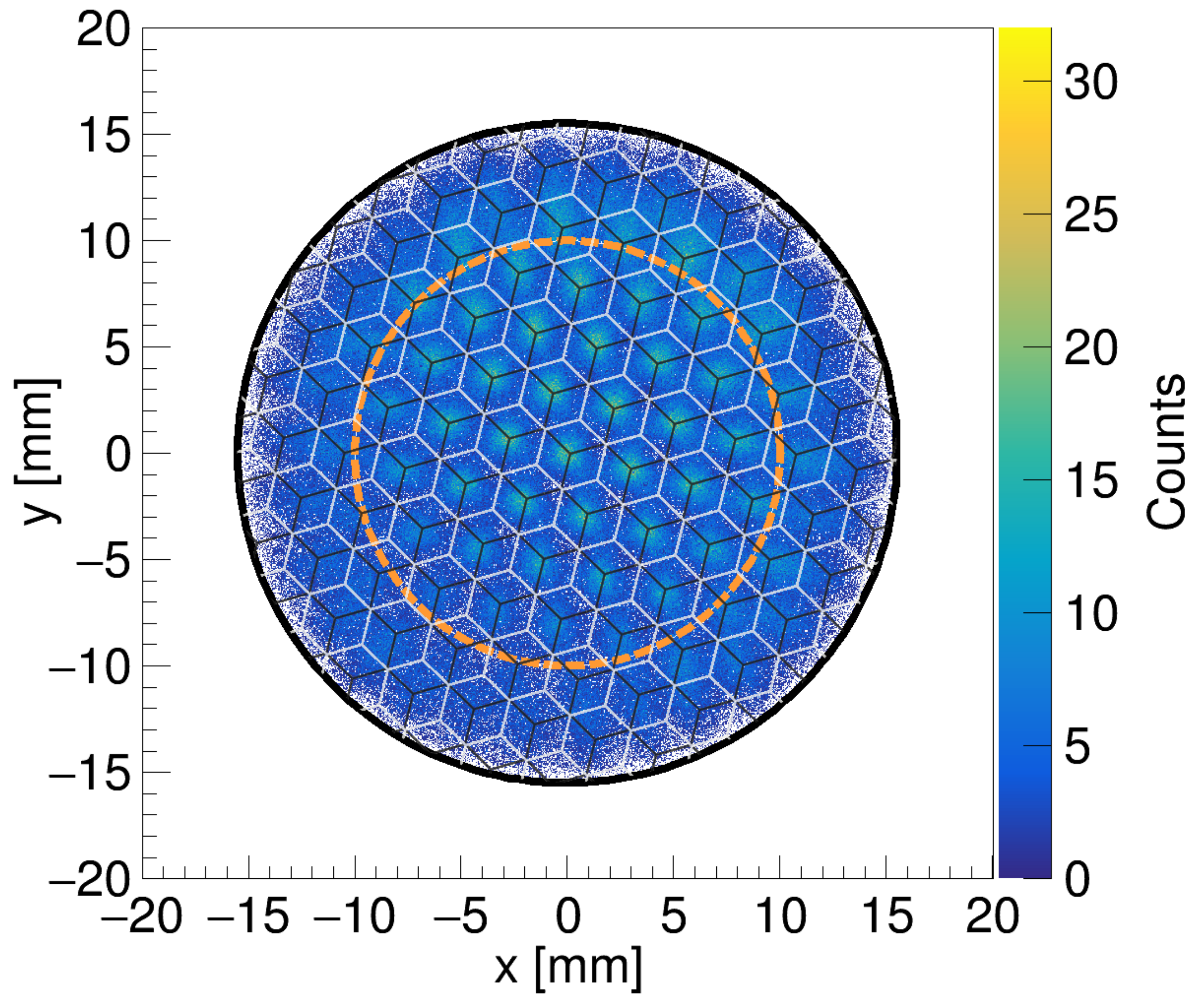

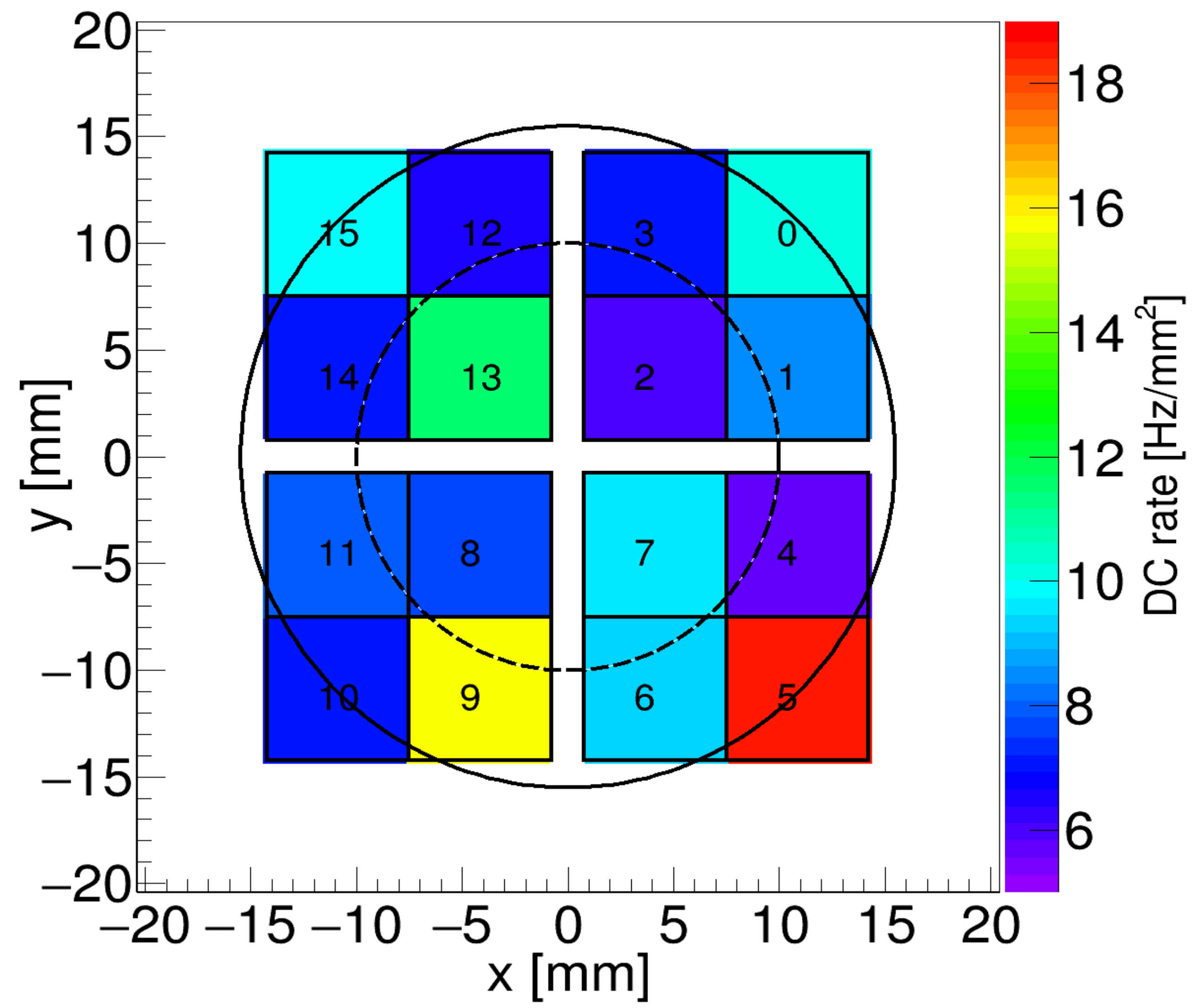

Characterisation with Internal Sources

- Mix keV-scale ER-sources with the xenon for homogeneous event distribution

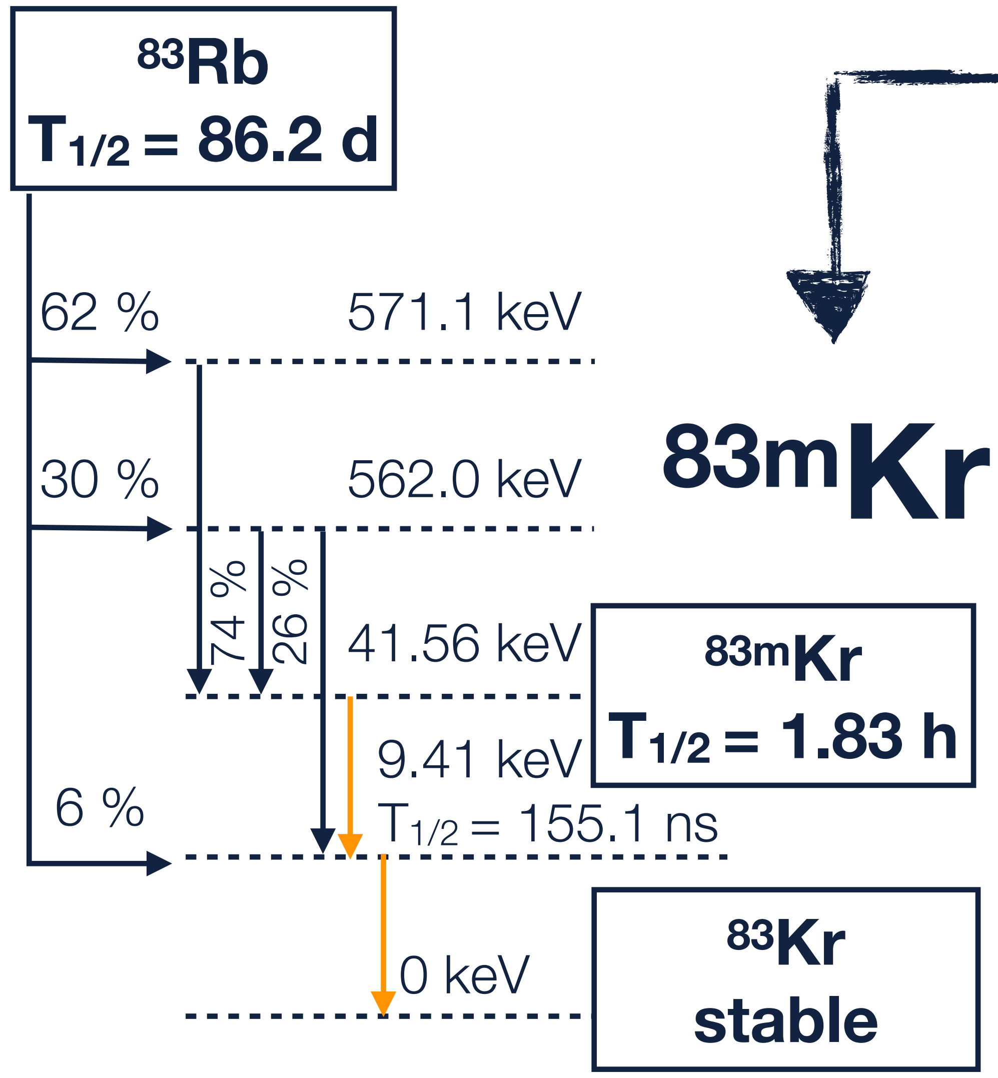

^{83m}Kr

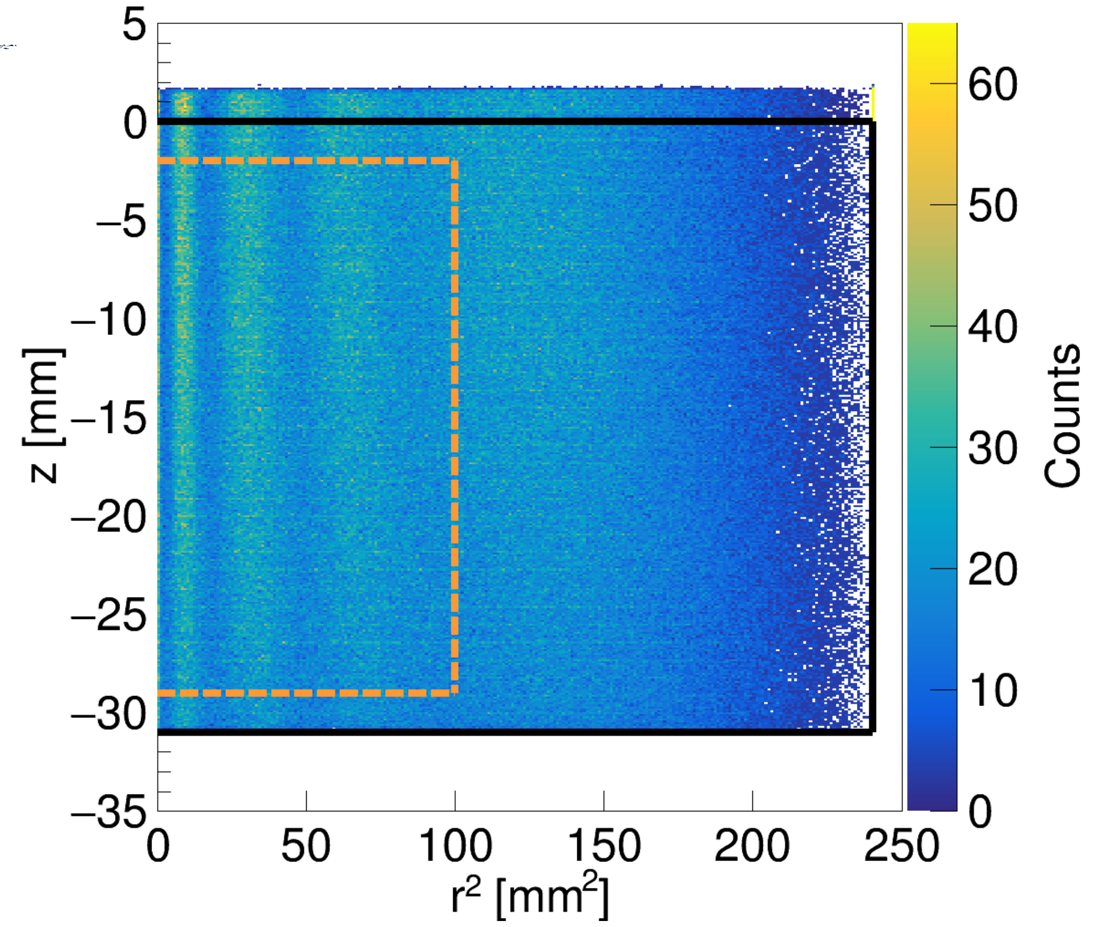

32.15 keV

9.41 keV

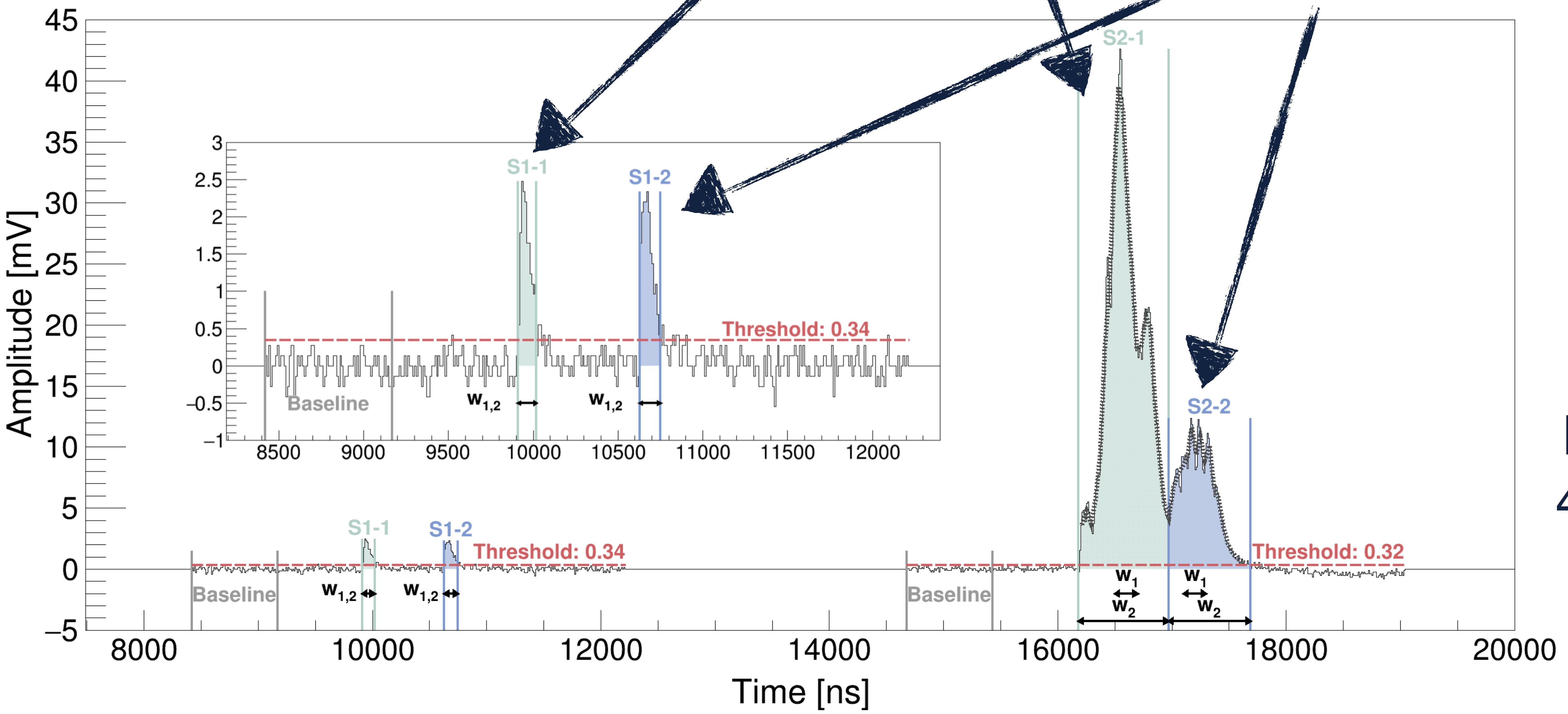

EPJ C 80, 477 (2020)

^{37}Ar

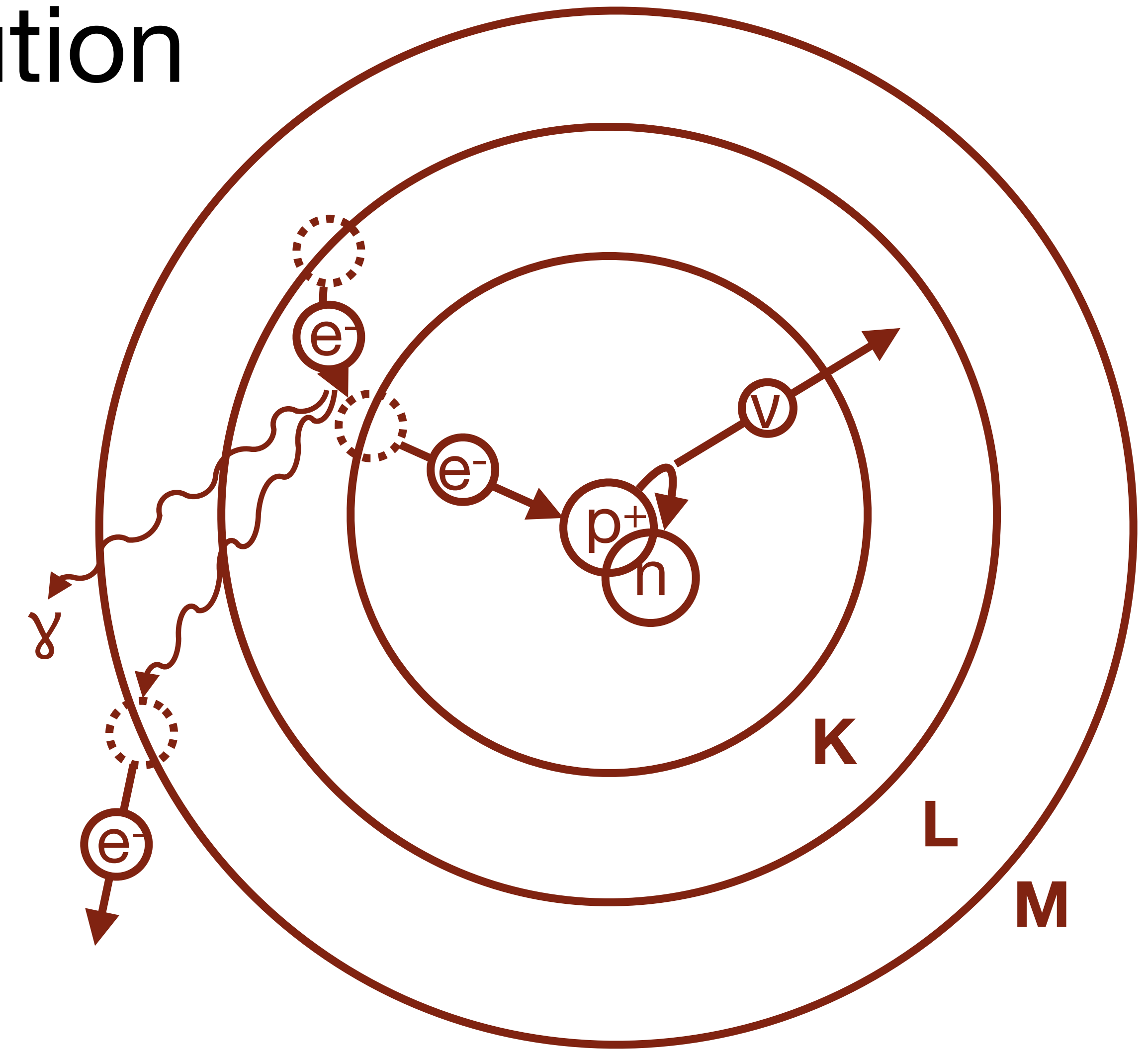

- ^{37}Ar $T_{1/2}$ = (35.01±0.02) days
- Electron capture: $e^- + {}^{37}Ar \longrightarrow {}^{37}Cl + \nu_e$

Decay mode	Energy release [keV]	Branching ratio
K capture	2.8224	90,17 %
L capture	0.2702	8,90 %
M capture	0.0175	0,93 %

^{83m}Kr Calibration

- Deploy a ^{83}Rb source
- ^{83m}Kr decays in two steps via isometric transition with intermediate $T_{1/2}$ = 155.1 ns

EPJ C 80, 477 (2020)

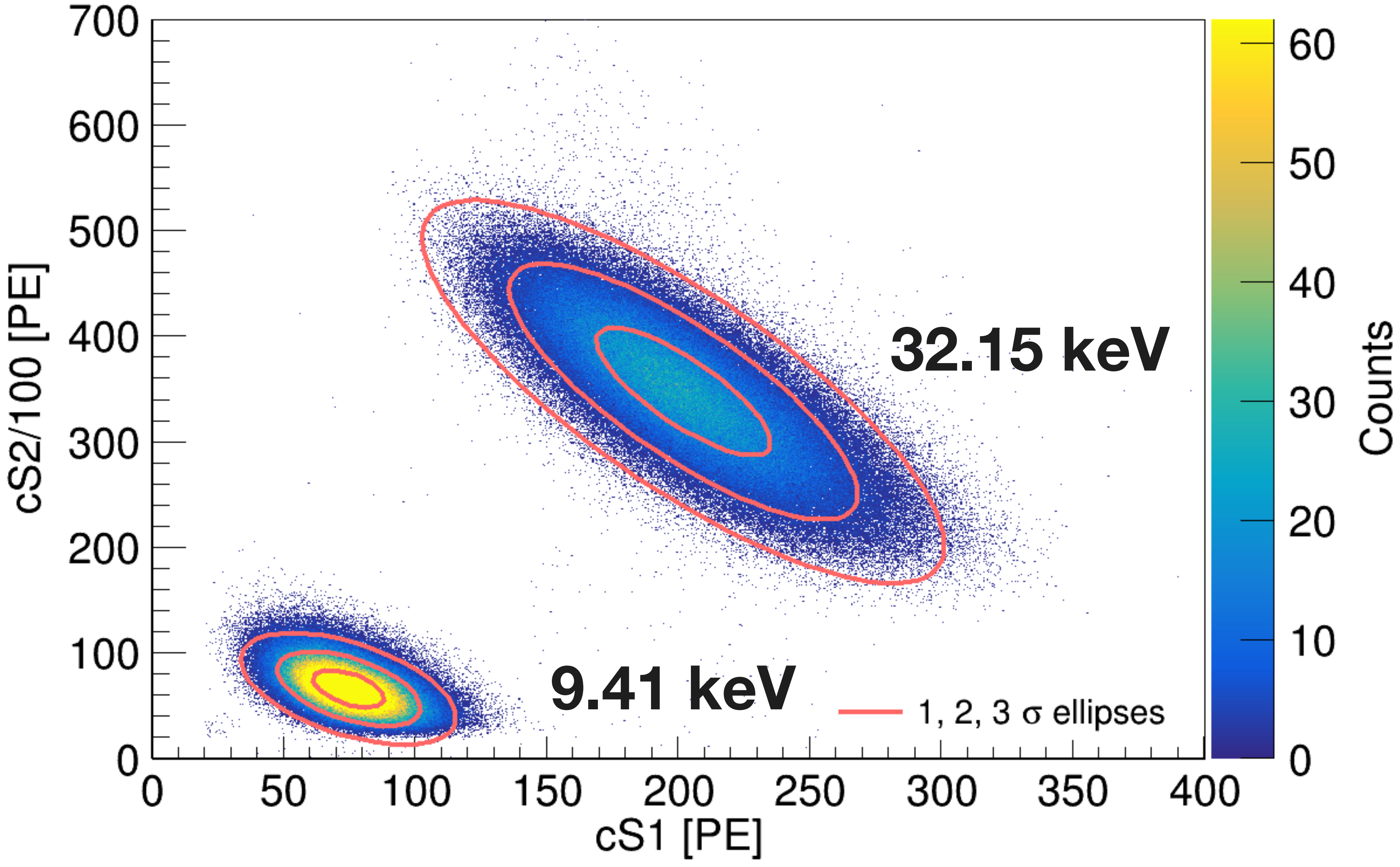

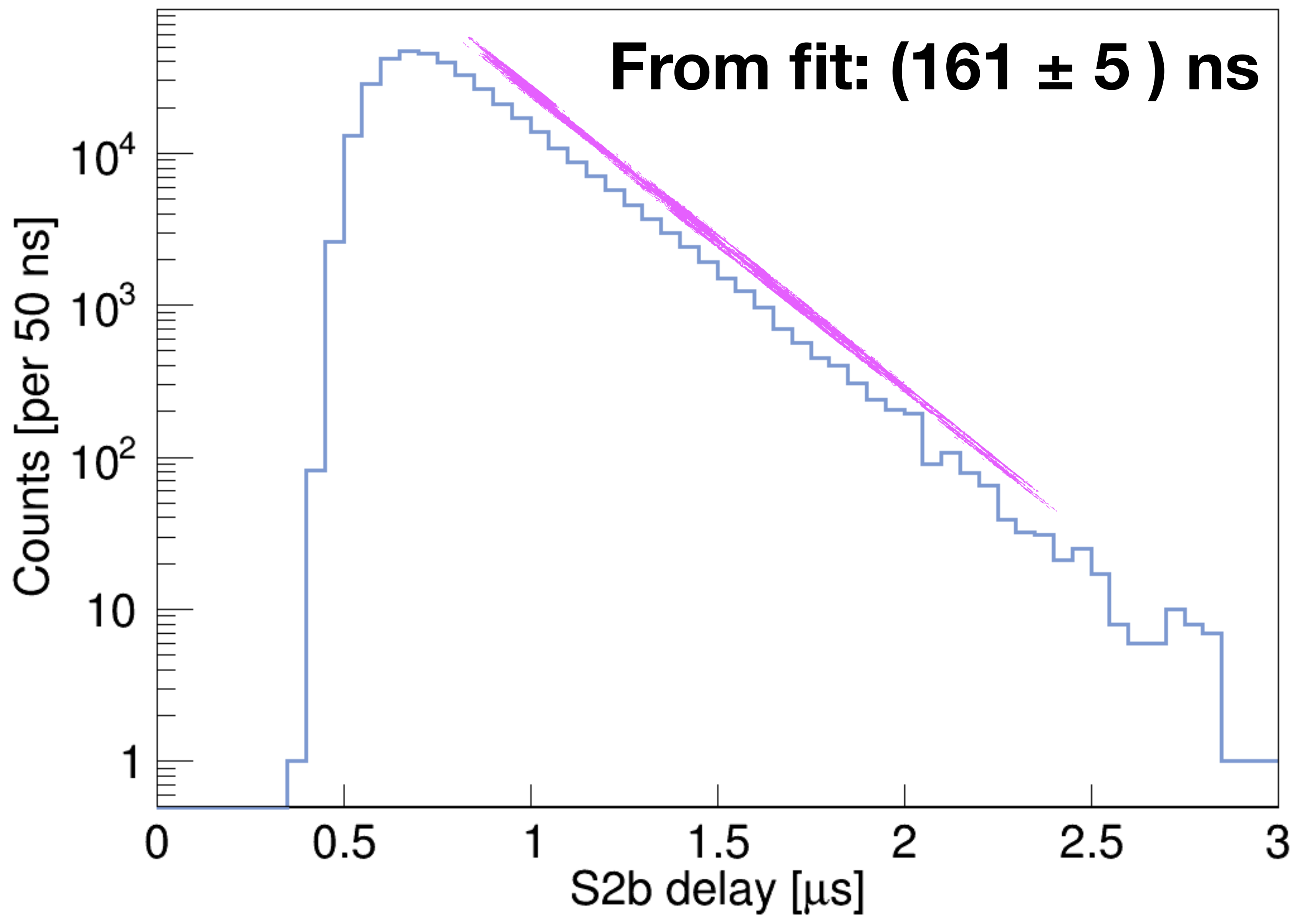

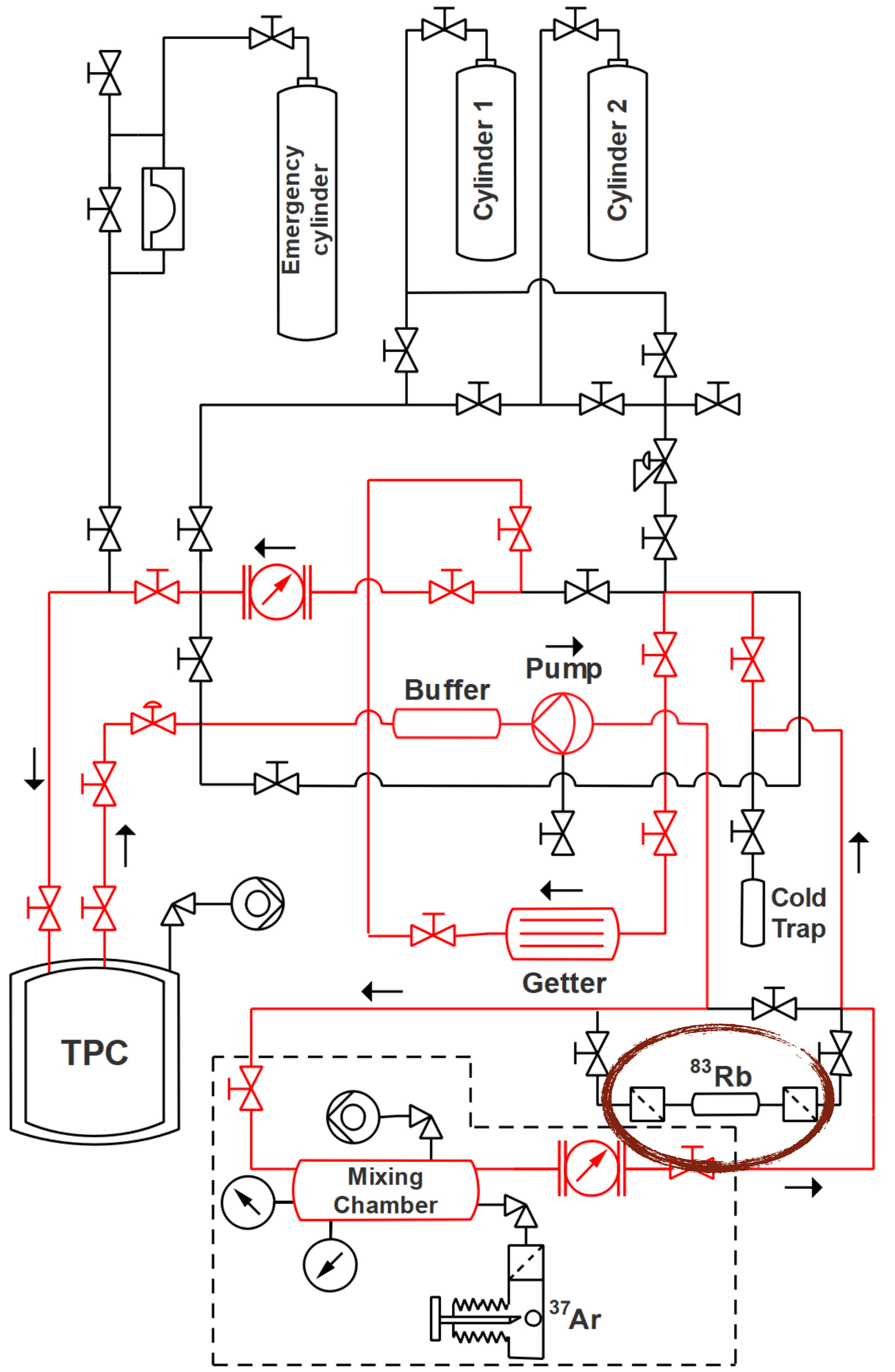

^{37}Ar Source Production and Introduction

- Production from natural Ar via thermal neutron capture on ^{36}Ar(n,ɣ) with ~5 barn
- Produced at Swiss Spallation Neutron Source (PSI Villigen): 10^{13} neutrons cm^{-2}s^{-1}

EPJ C 80, 477 (2020)

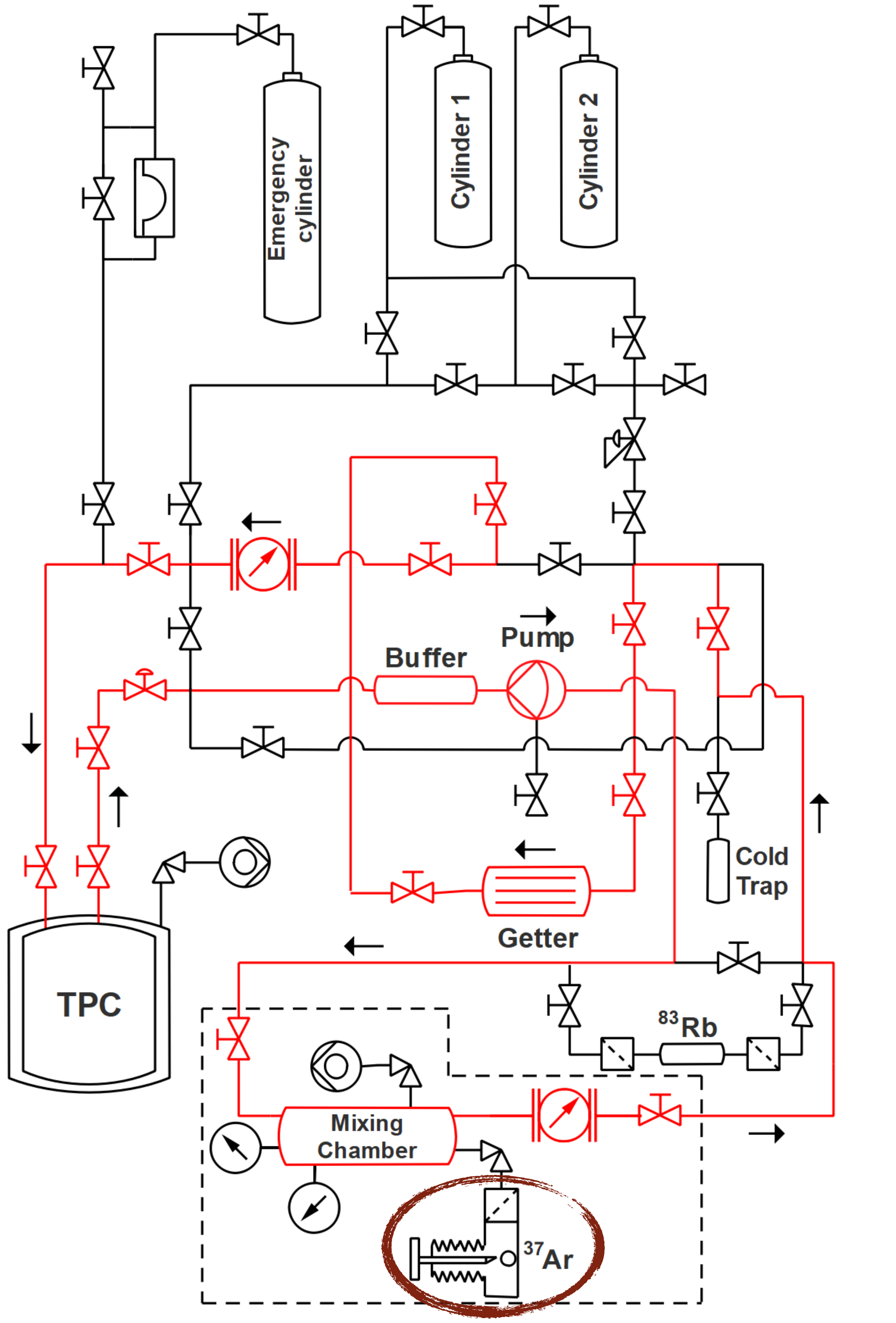

Isotope*	Abundance [%]	$T_{1/2}$	Decay mode	Daughter	Energy [keV]	Activity** [kBq]
^{36}Ar	0.334	-	stable	-	-	-
^{37}Ar	syn	35.01 d	ε	^{37}Cl	0.0175 – 2.82	20
^{38}Ar	0.063	-	stable	-	-	-
^{39}Ar	trace	268 y	β^-	^{39}K	Q-value: 565	2×10^{-4}
^{40}Ar	99.604	-	stable	-	-	-
^{41}Ar	syn	109.6 min	β^-	^{41}K	Q-value: 2492	$< 10^{-3}$

*higher isotopes negligible due to small $T_{1/2}$ or low activity
**calculated per 1.5 cm^2 quartz ampule

^{37}Ar Calibration

- Identified K- and L-shell population
- Checked half-life and branching ratio
- Derived detector response parameters: $g1 := S1/n_\gamma\ ,\ \ g2 := S2/n_{e^-}$
- Compared light and charge yield to NEST predictions

EPJ C 80, 477 (2020)

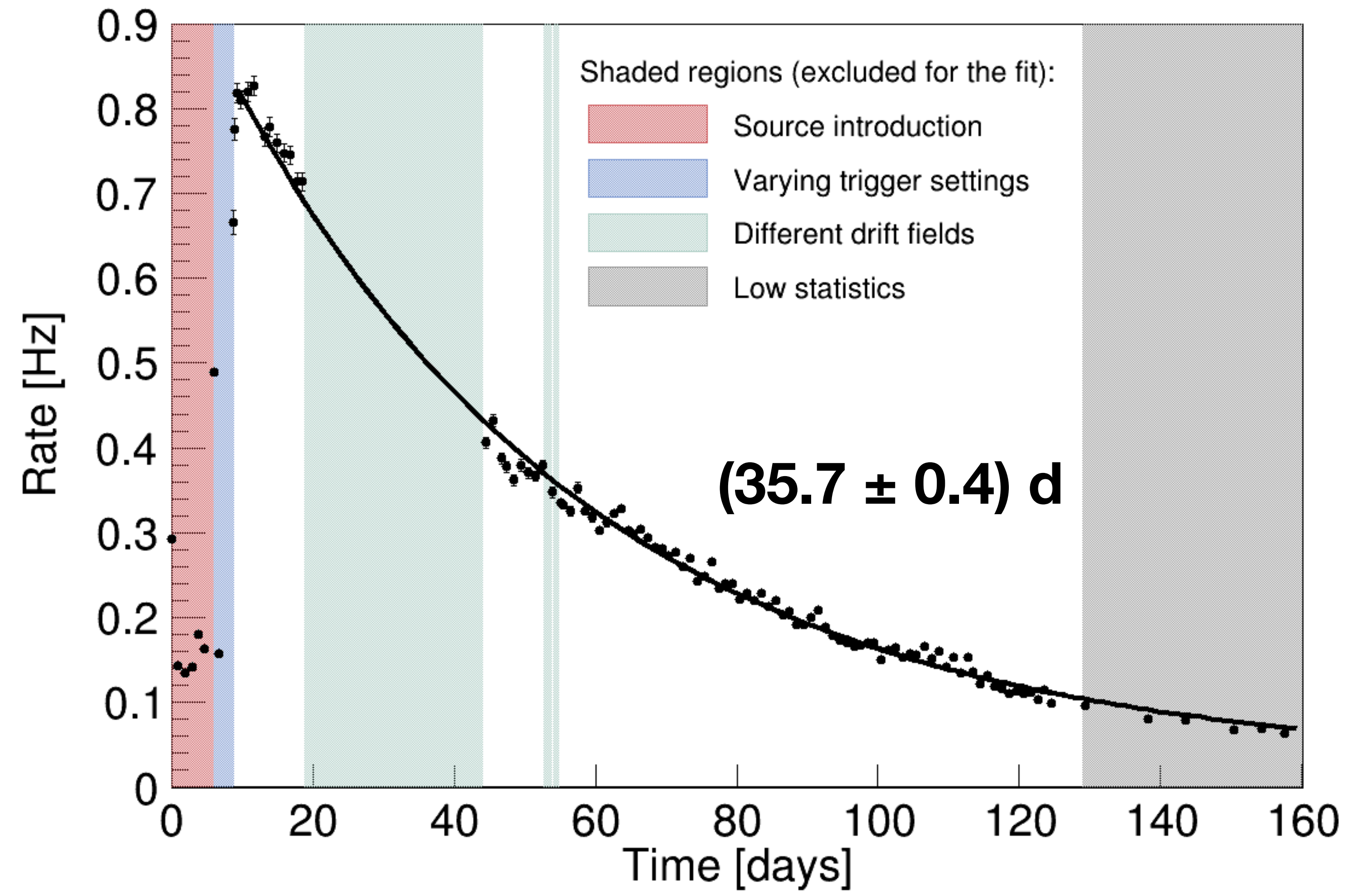

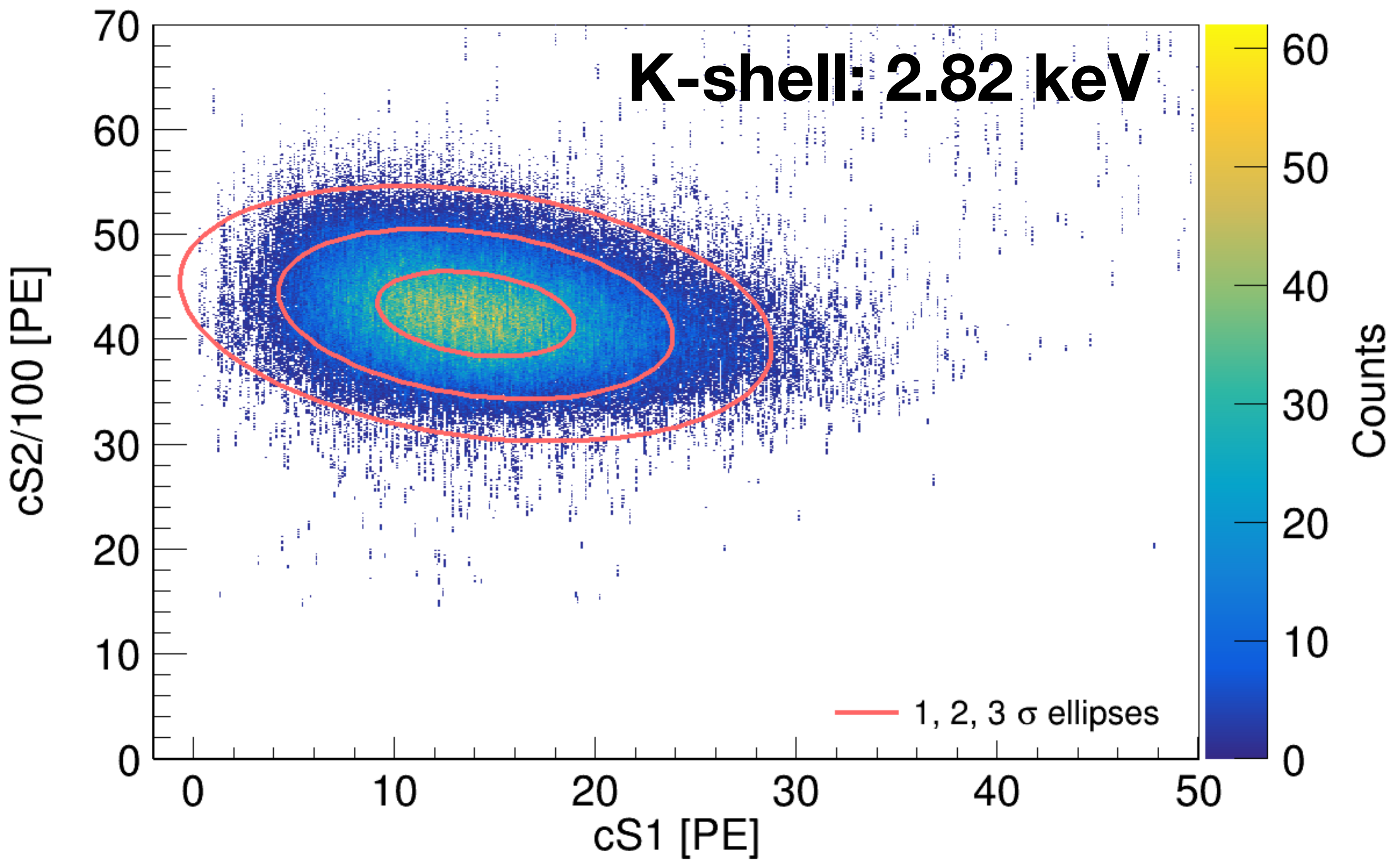

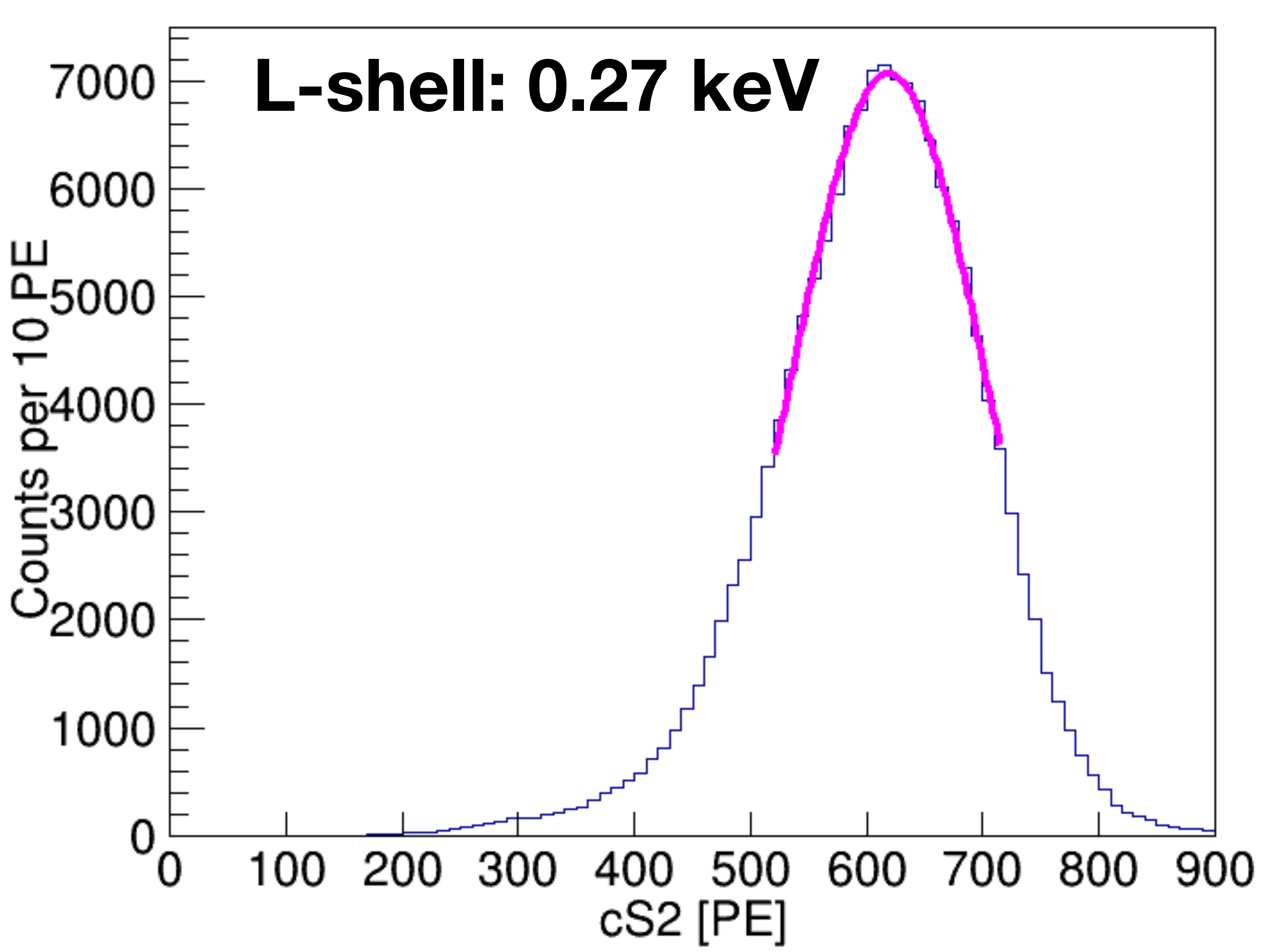

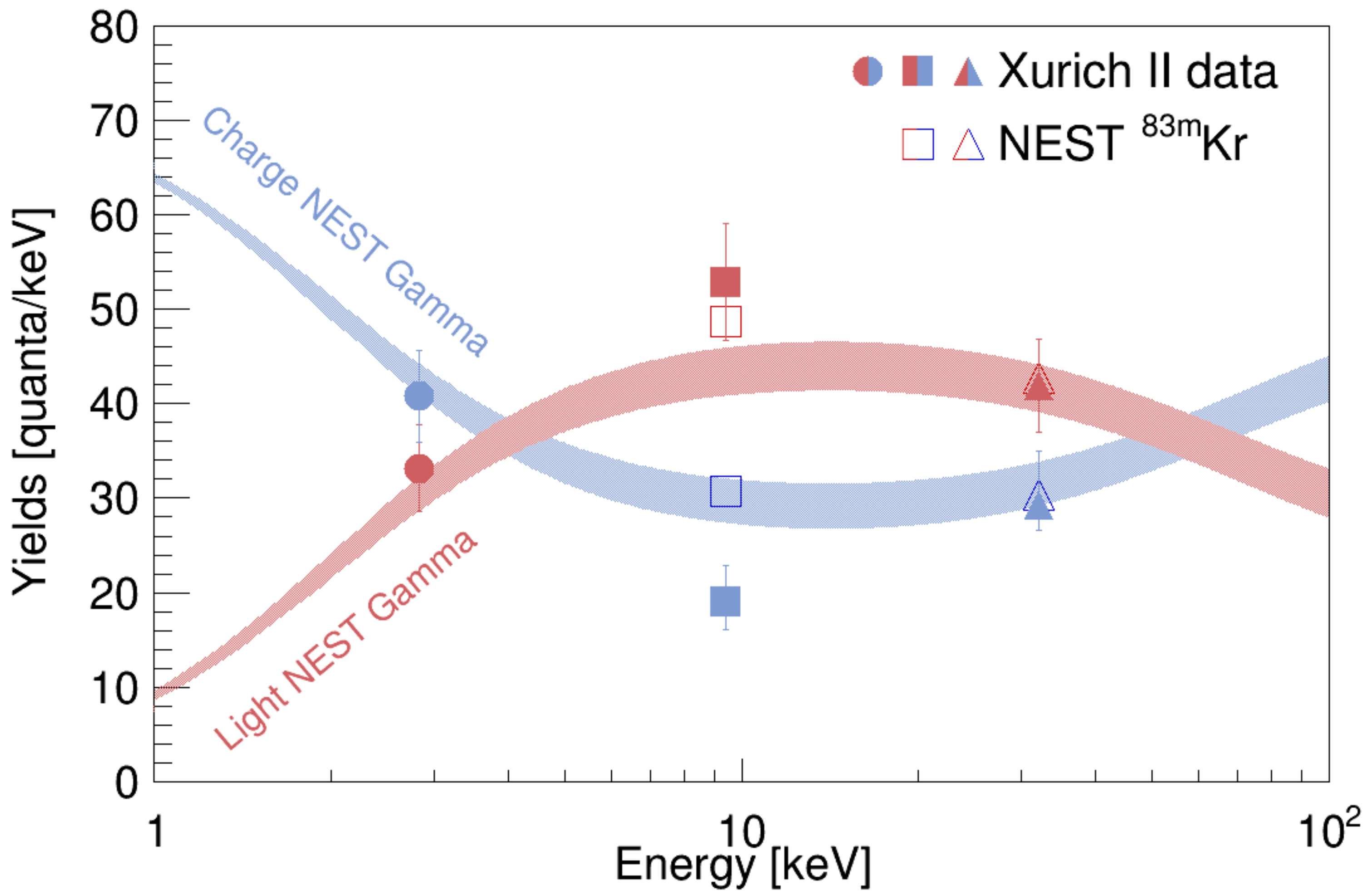

Given: High-statistics keV-scale calibration data in dual-phase mode at different drift fields

Determine: W-value

Solution: ?

Measurement Principle

- Rewriting $E = (n_\gamma + n_{e^-})W$ with the detector gains $g1 := S1/n_\gamma$, $g2 := S2/n_{e^-}$:

Local: $W = g2 \dfrac{E}{\frac{g2}{g1} S1 + S2}$

- Slope of anti-correlation line
- S1-S2 population at energy E
- Independent measurement of g2

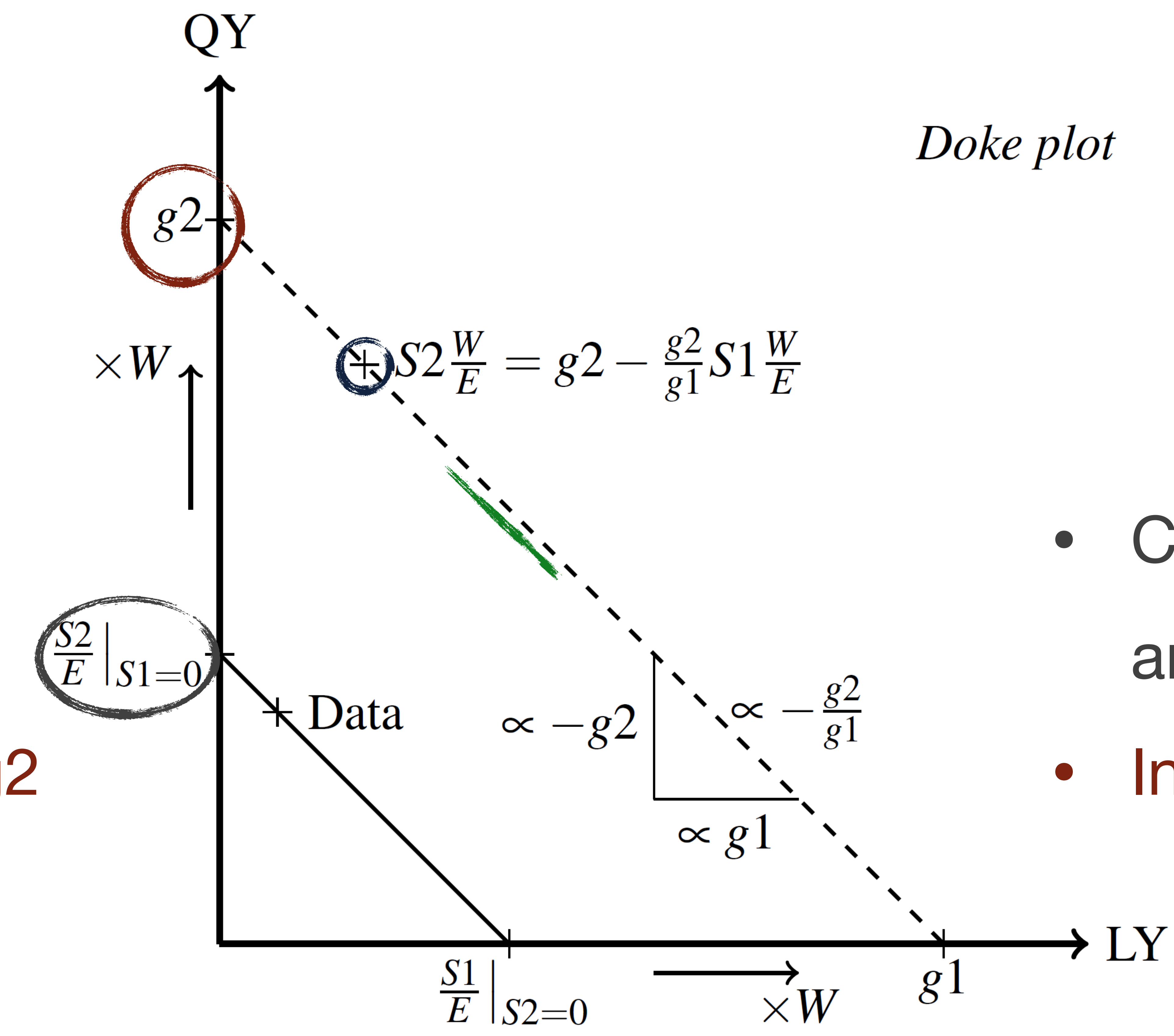

Global: $W = g2 \dfrac{E}{S2}\Big|_{S1=0}$

- Charge yield axis intercept of anti-correlation line
- Independent measurement of g2

Problem: How to determine g2 in an absolute way?
Idea: When a single electron is extracted to the gas phase: g2=S2

Single Electron Gain Measurement

- For single electron extraction (SE): g2=S2
- Highly abundant, quantised process with a rate of ~17 Hz
- Origin: delayed extraction, trapped charges, cathode emission, ^{37}Ar M-shell (max. 0.5 %)
- Detection and S1/S2 identification efficiencies relevant for small S2s

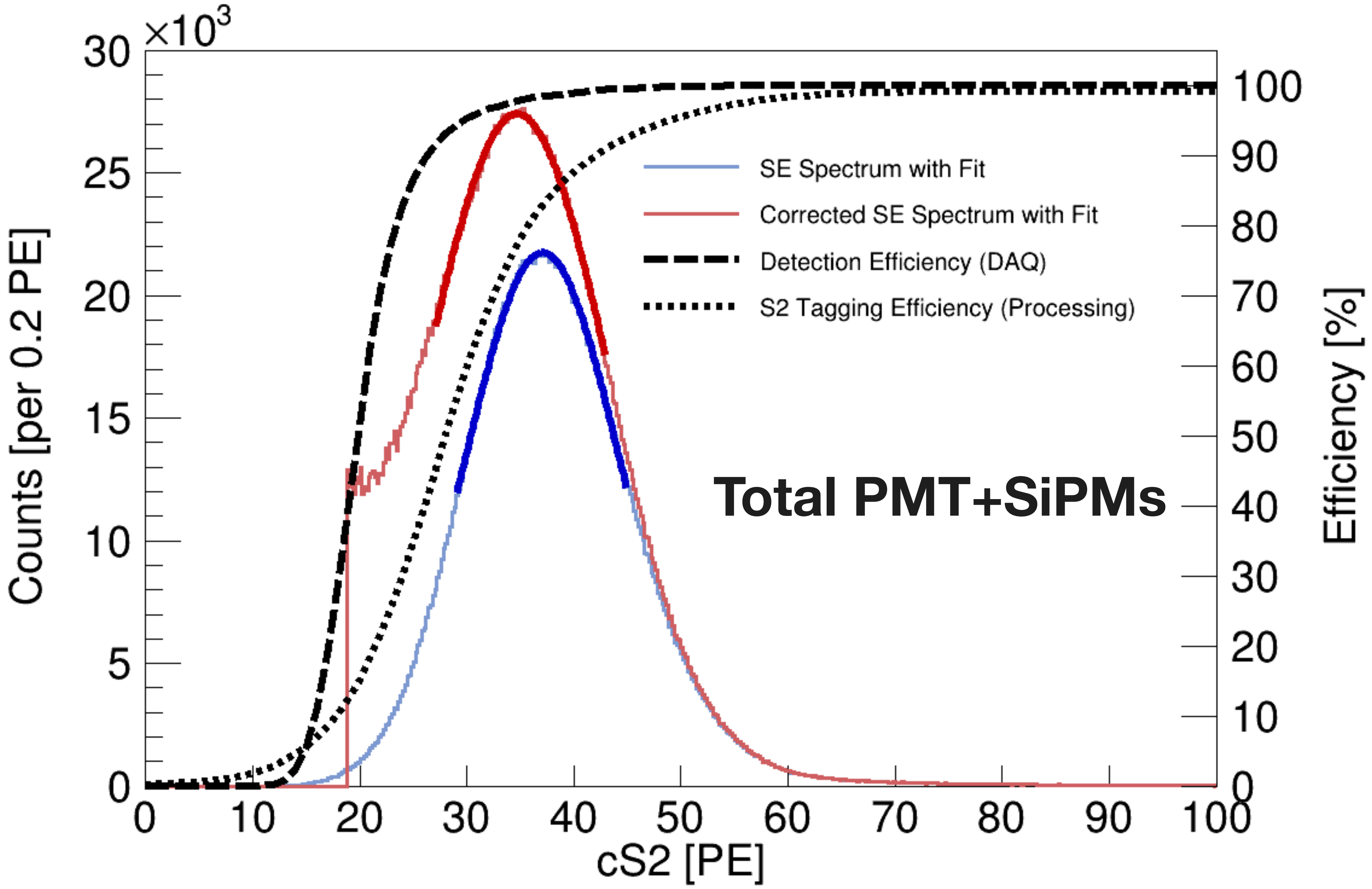

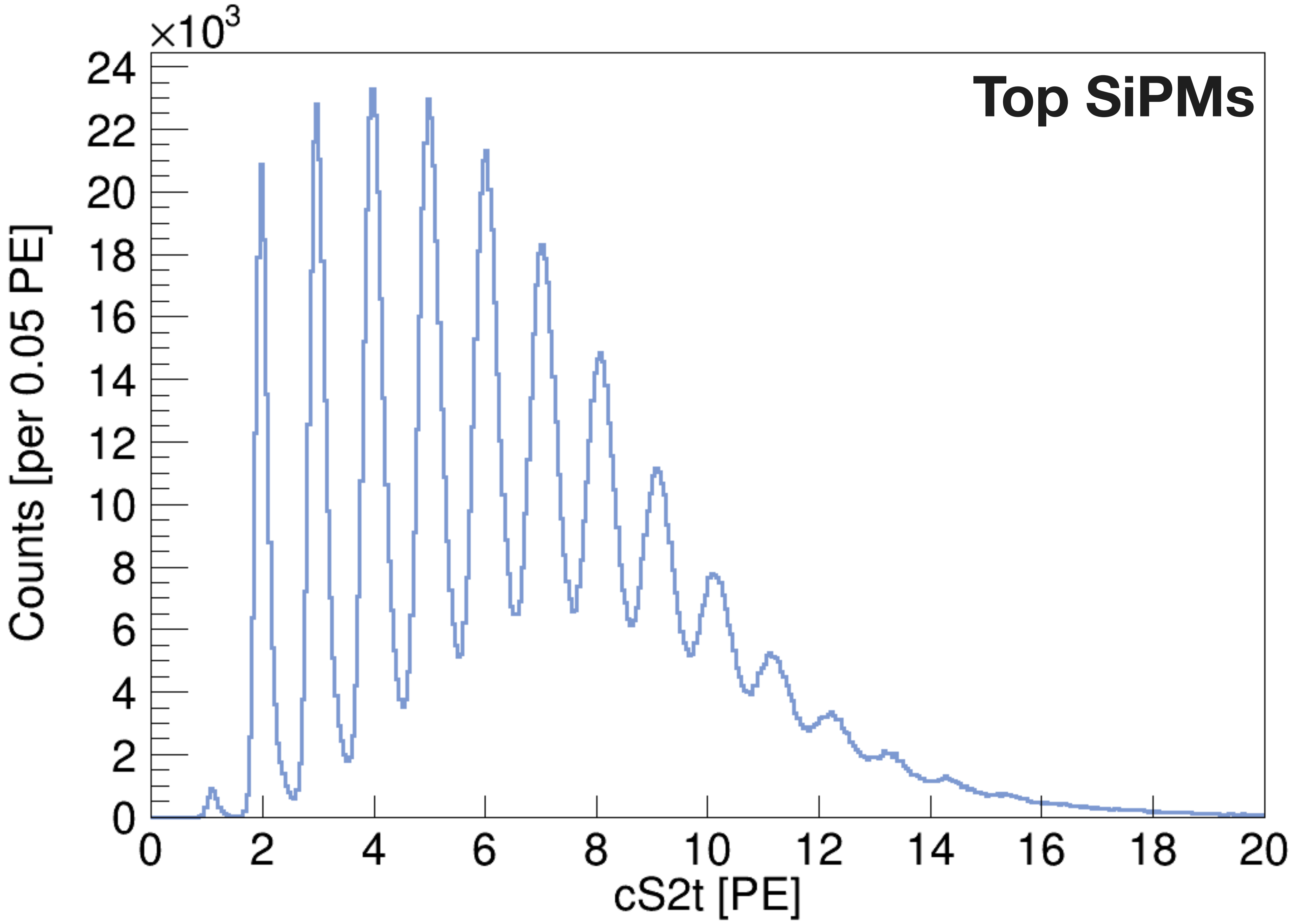

➡ DPE/crosstalk and efficiency corrected: $\mathbf{g2 = (29.84 \pm 0.01\,(stat.) \pm 0.40\,(syst.))\,PE/e-}$

Anti-Correlation Fit Parameters

- Use anti-correlation fit for 2.82 keV, 9.41 keV, 32.15 keV, 41.56 keV at all available drift fields (from 80 (484) to 968 V/cm for ^{37}Ar (^{83m}Kr)) -> better accuracy for higher separation in S1/S2

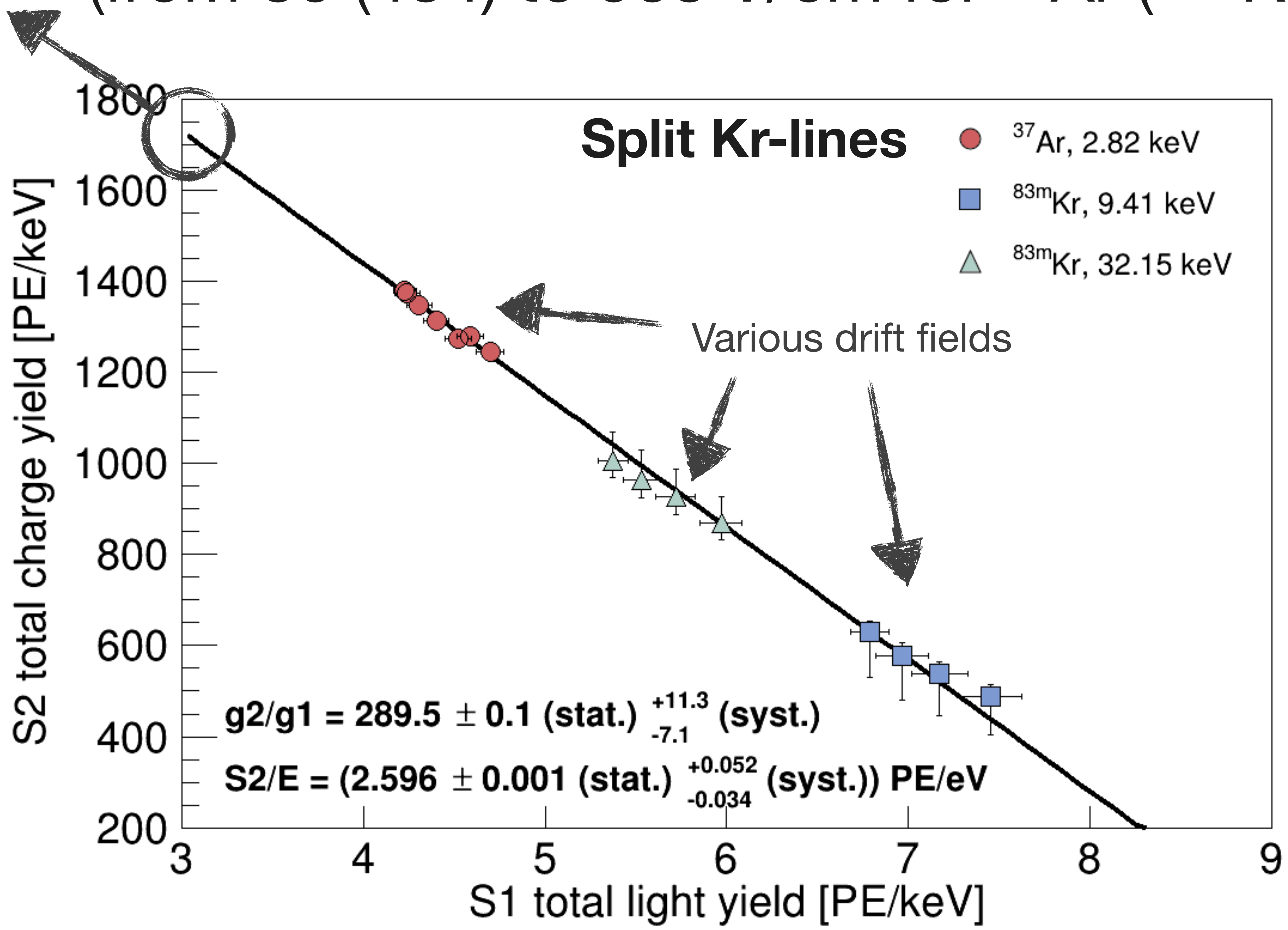

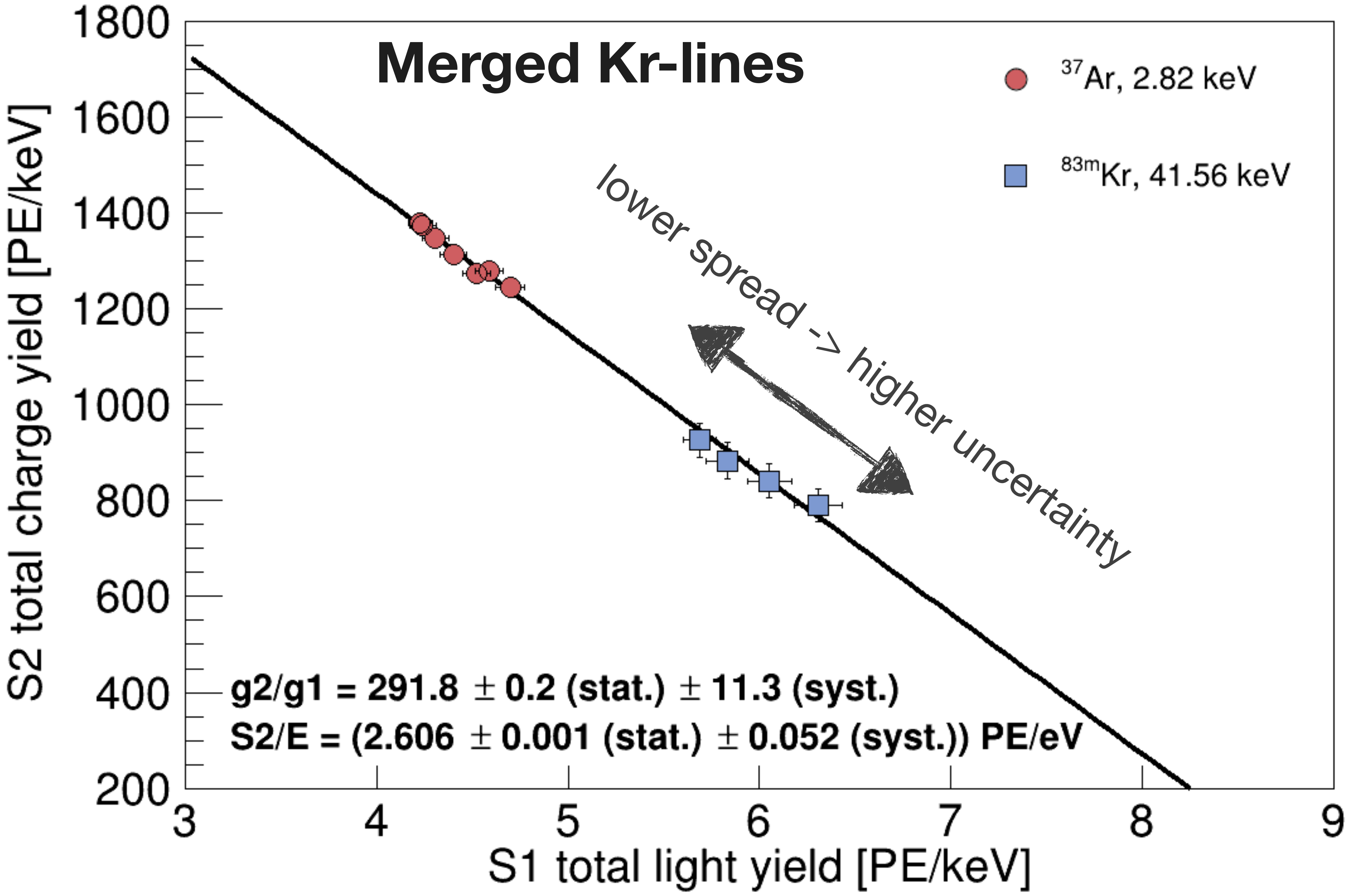

➡ DPE/crosstalk corrected: $\mathbf{g2/g1 = 289.5 \pm 0.1\,(stat.)^{+11.3}_{-7.1}\,(syst.)}$,

$\mathbf{S2/E = (2.596 \pm 0.001\,(stat.)^{+0.052}_{-0.034}\,(syst.))\ PE/eV}$

Systematic Uncertainties

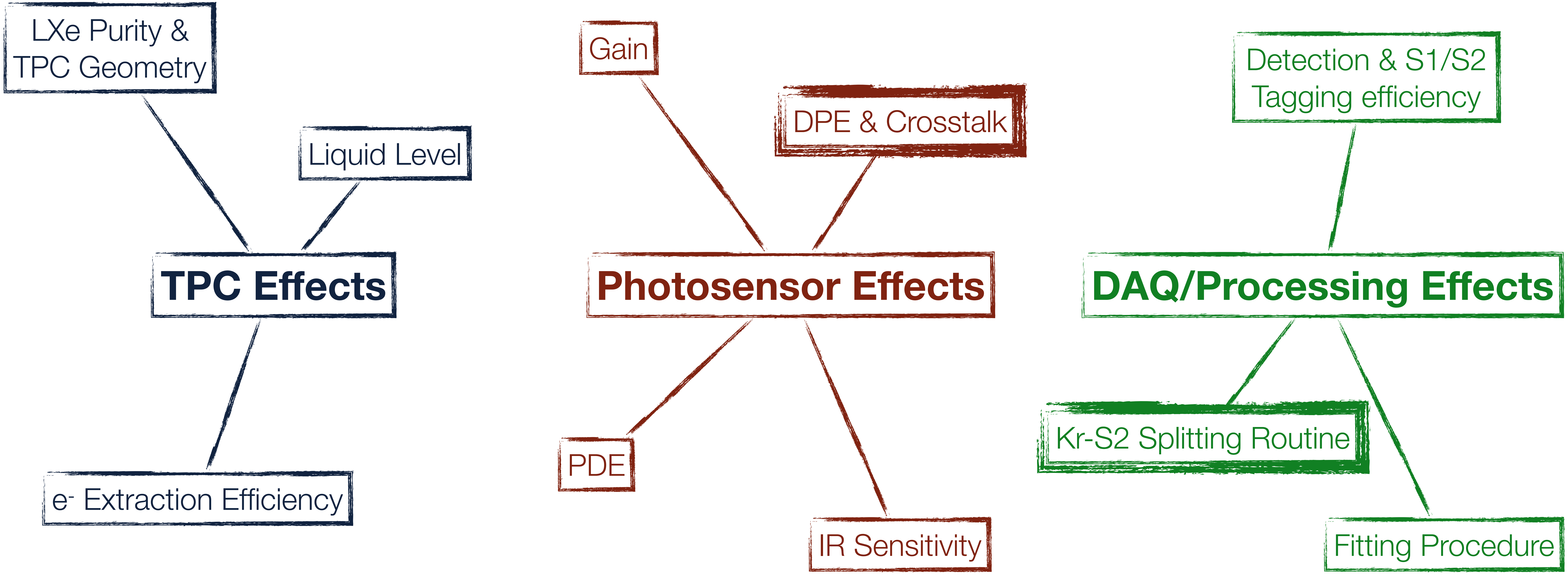

Photosensor Effects

SiPM Double Photoelectron Emission

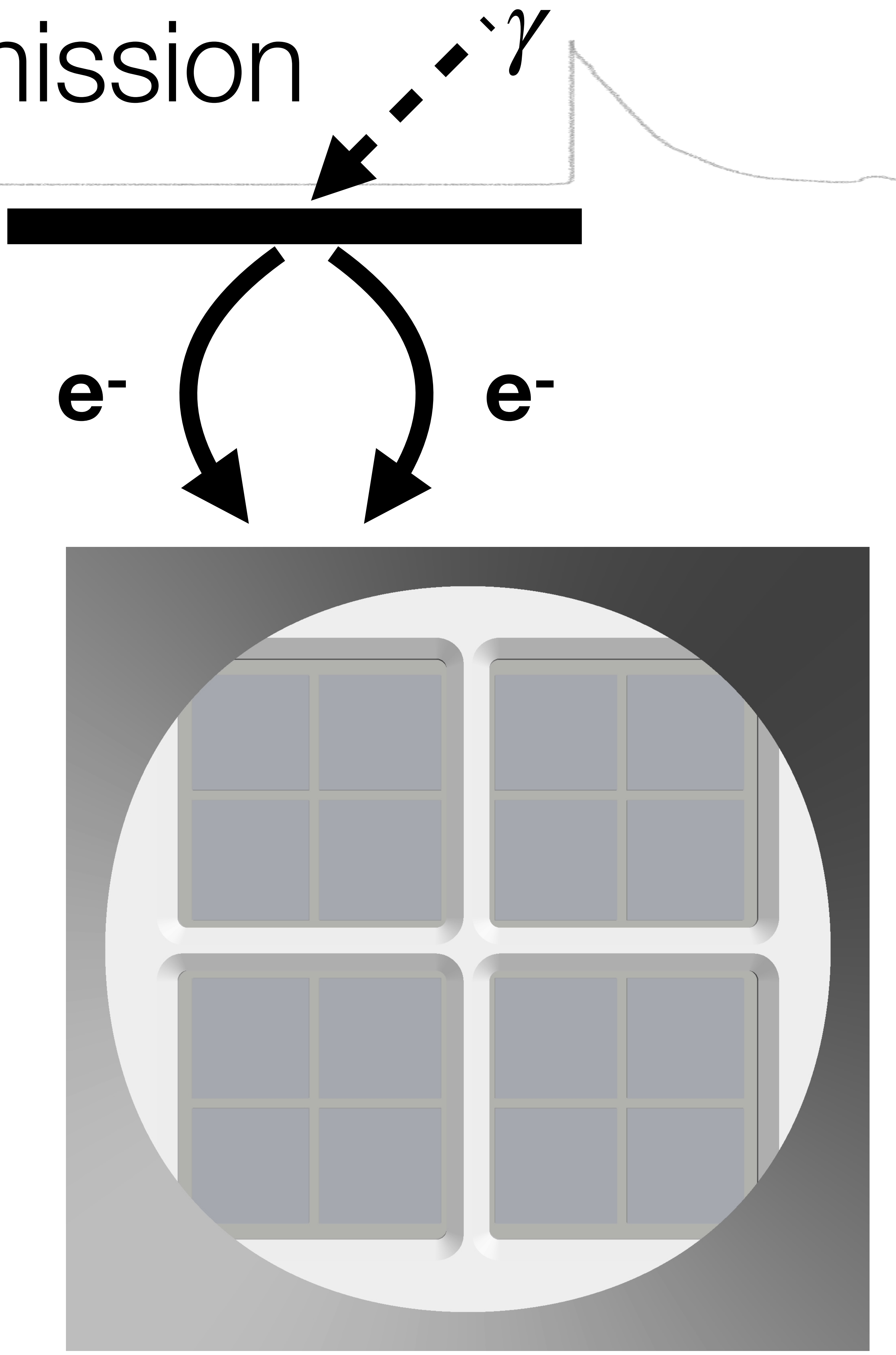

- Well-known for PMTs, typically ~20 % [3–5]
- Single-cell output should be the same?
- Well-known for SiPMs: crosstalk among neighboring cells -> photon crosses trenches, 2.1 % at 4 V OV and 3.3 % at 5 V OV [6]
- But: crosstalk measured as ratio of 1.5 PE and 0.5 PE threshold from DC data -> excitations from the bulk, not external -> Any difference?
- Single photon source not available -> position cut doesn't work in small TPC -> Use combinatorial method instead

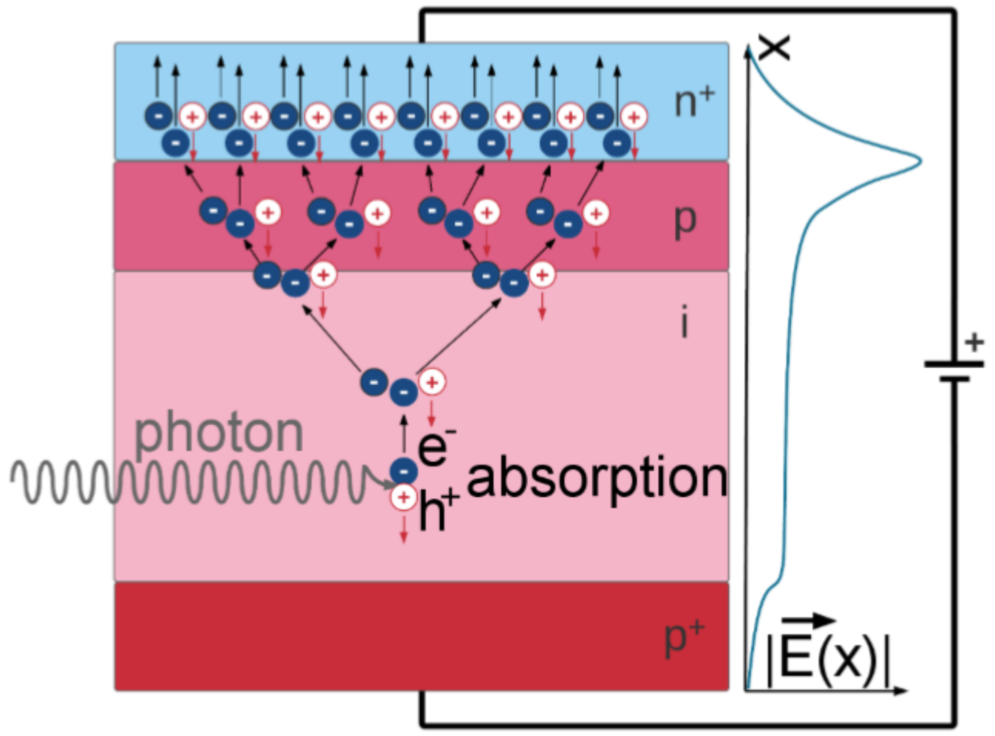

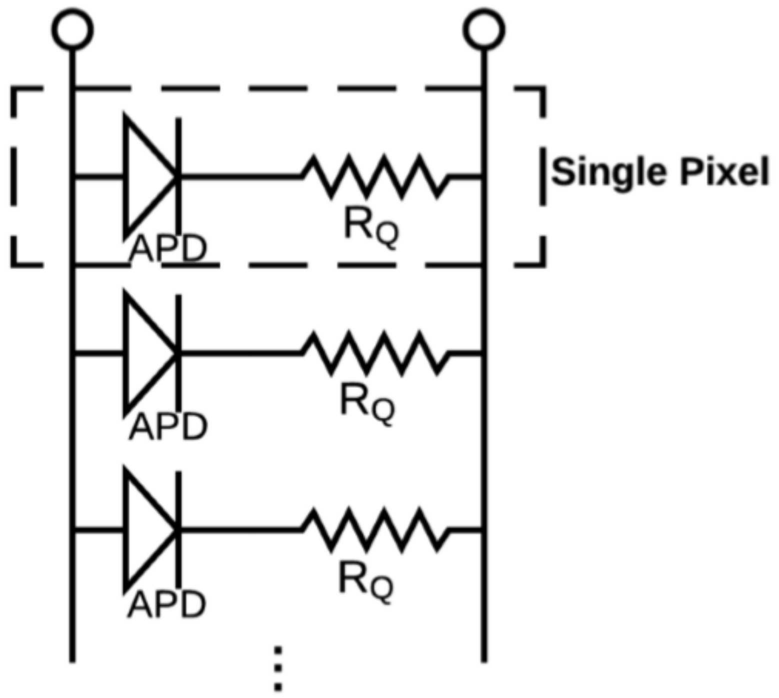

[3] C.H. Faham et al., JINST 10 P09010 (2015)
[4] P. López Paredes et al., Astropart. Phys 102 56–66 (2018)
[5] E. Aprile et al., Phys. Rev. D 99, 112009 (2019)
[6] L. Baudis et al. JINST 13 P10022 (2018)

Photosensor Effects

A Combinatorial Approach

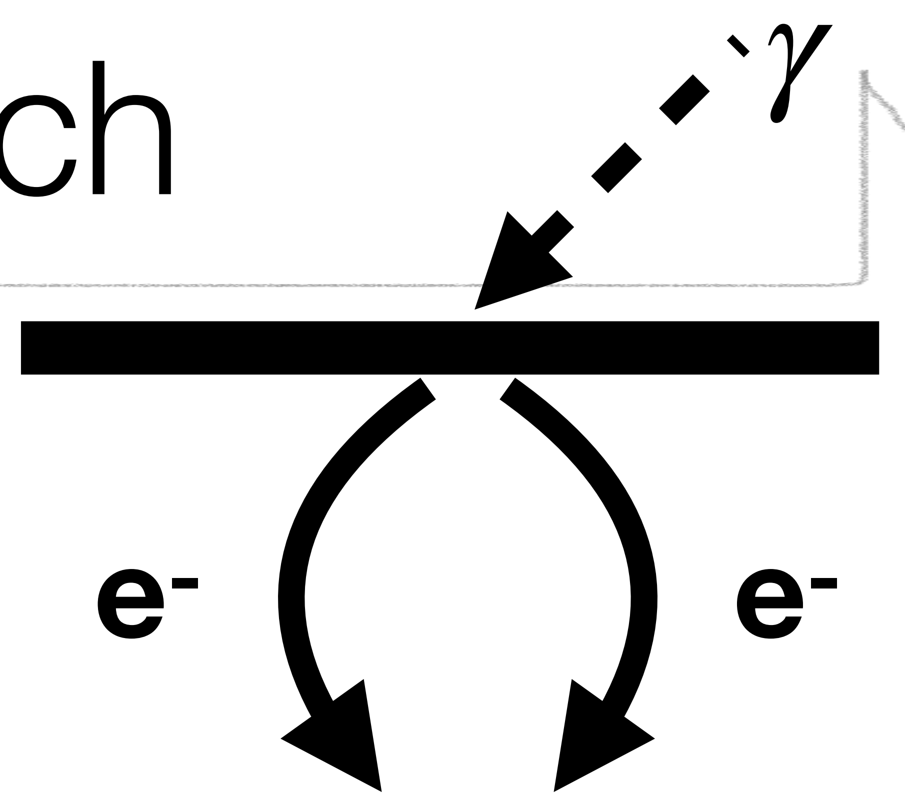

- p_i…mean light fraction of sensor i for FV
- k_i…number of hits in sensor i
- q…DPE probability
- Consider events with 3 detected hits -> 3 cases:

I. $$k_i = 3, k_j = 0\, \forall j \neq i$$

$$3\,\gamma \rightarrow 3\,\text{hits} \quad \text{or} \quad 2\,\gamma \rightarrow 3\,\text{hits} \quad \text{or} \quad 1\,\gamma \rightarrow 3\,\text{hits*}$$

➡ *NNLO

➡ not accessible, because very unlikely

II. $$k_i = 2, k_l = 1, k_j = 0\, \forall j \neq l \neq i$$

$$3\,\gamma \rightarrow 2+1\,\text{hits} \quad \text{or} \quad 2\,\gamma \rightarrow 2+1\,\text{hits}$$

➡ $$N^{\text{II}} = N_{3\,\gamma} \cdot 3 \sum_{i=0}^{15} p_i^2(1-p_i) + N_{2\,\gamma}^{2\text{s}} \cdot 2q(1-q)$$

III. $$k_i = k_l = k_m = 1, k_j = 0\, \forall j \neq l \neq m \neq i$$

$$3\,\gamma \rightarrow 1+1+1\,\text{hits}$$

➡ $$N^{\text{III}} = N_{3\,\gamma} \cdot \sum_{i=0}^{15} \sum_{j\neq i} p_i p_j (1-p_i-p_j)$$

$N_{3\gamma}$…# events with 3 initial photons that are all detected

$N_{2\gamma}^{2\text{s}} = \dfrac{N^{2\text{h},2\text{s}}}{(1-q)^2}$…# events with 2 initial photons detected by two different sensors

$N^{2\text{h},2\text{s}}$…# events with total 2 hits, one in each sensor

A Combinatorial Approach

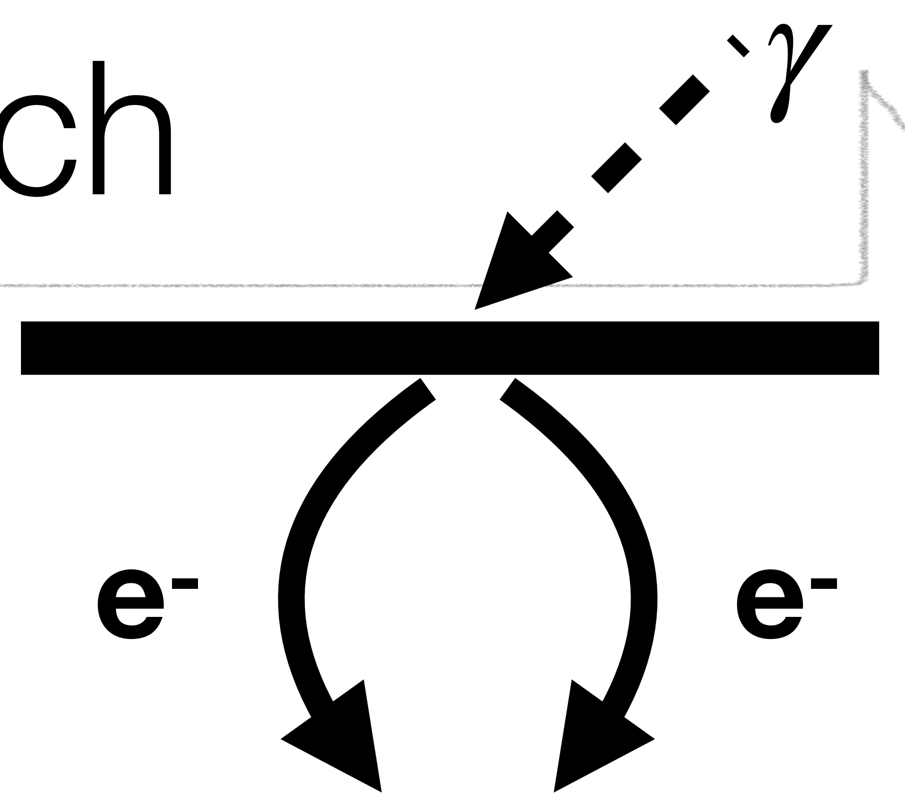

- $$q = \frac{\tilde{N}}{2N^{2\mathrm{h},2\mathrm{s}} + \tilde{N}}, \qquad \tilde{N} := N^{\mathrm{II}} - N^{\mathrm{III}} \frac{3\sum_{i=0}^{15} p_i^2(1-p_i)}{\sum_{i=0}^{15}\sum_{j\neq i} p_i p_j (1 - p_i - p_j)}$$
- Light fractions in the sensors from data (simulation):
- Corners: 4.6 % (5.4 %)
- Edges: 6.2 % (6.2 %)
- Middle: 8.0 % (7.2 %)
- From SE spectra: **q = (2.2 ± 0.1) %**
- Well in agreement with the crosstalk probability from DC data (Baudis et al., JINST 13 (2018) P10022)
- No extra DPE effect for SiPMs

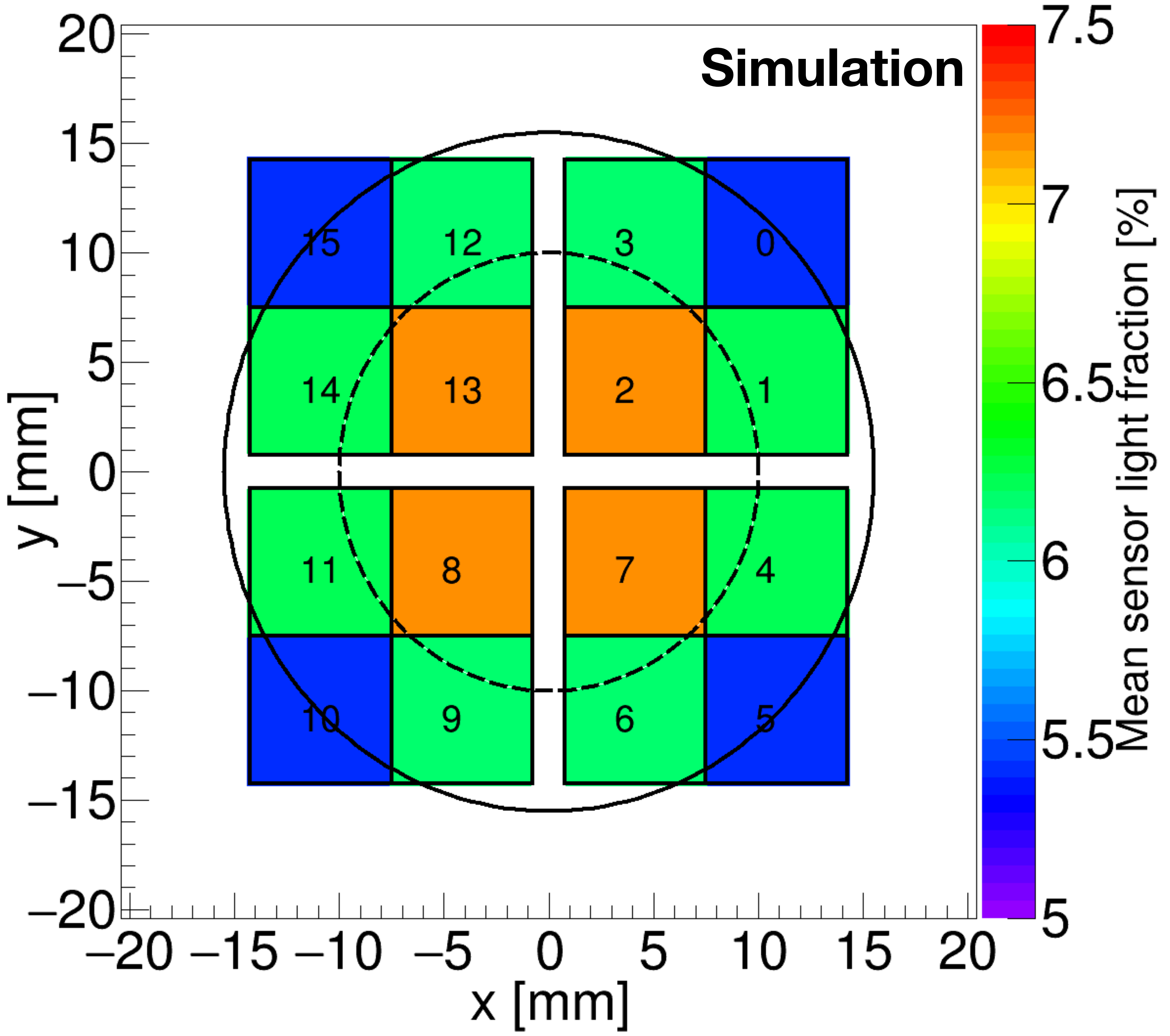

DAQ/Processing Effects

Kr-S2 Splitting Routine

- Split at local intermediate minimum when waveform has fallen below half the maximum height of the two peaks

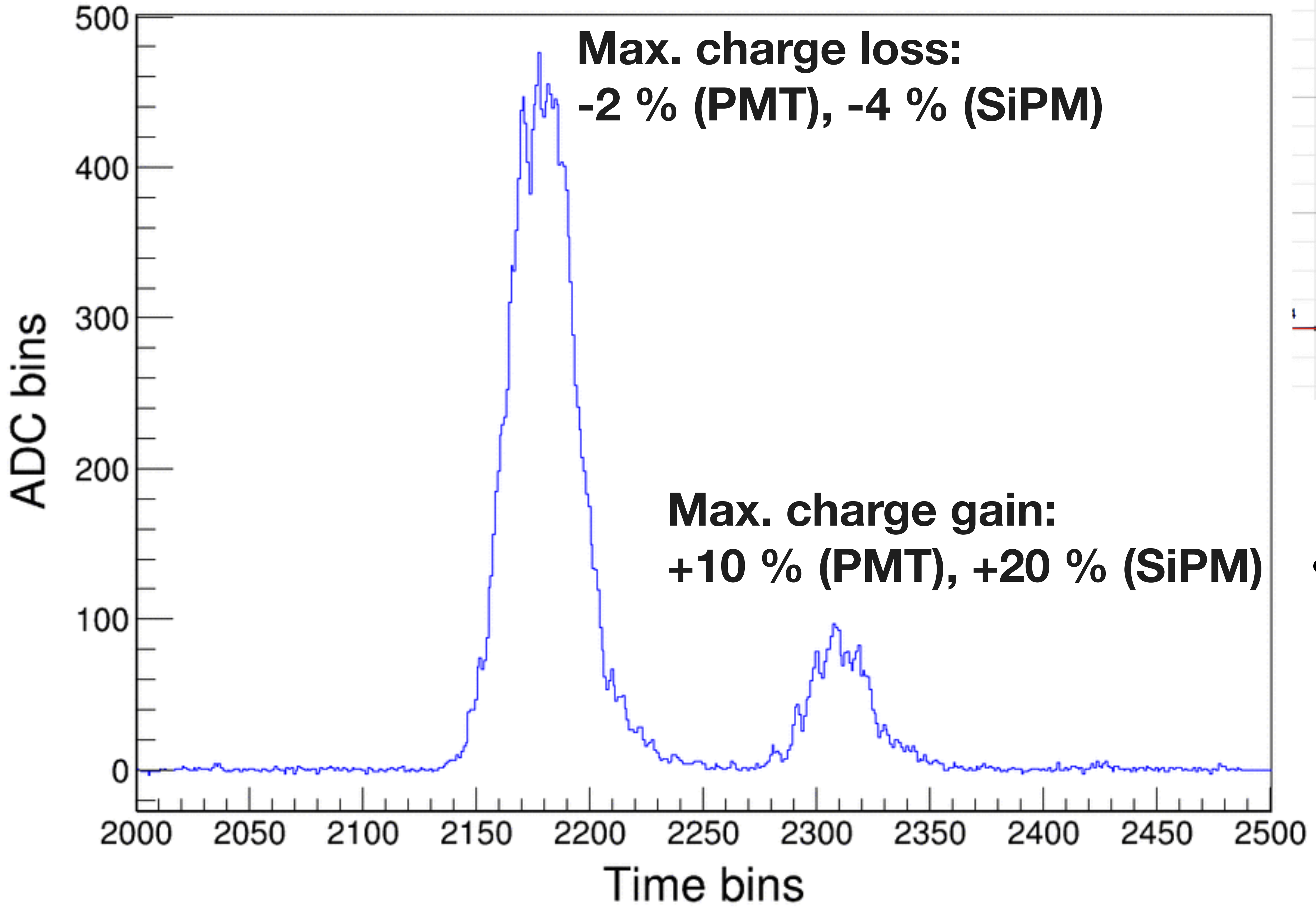

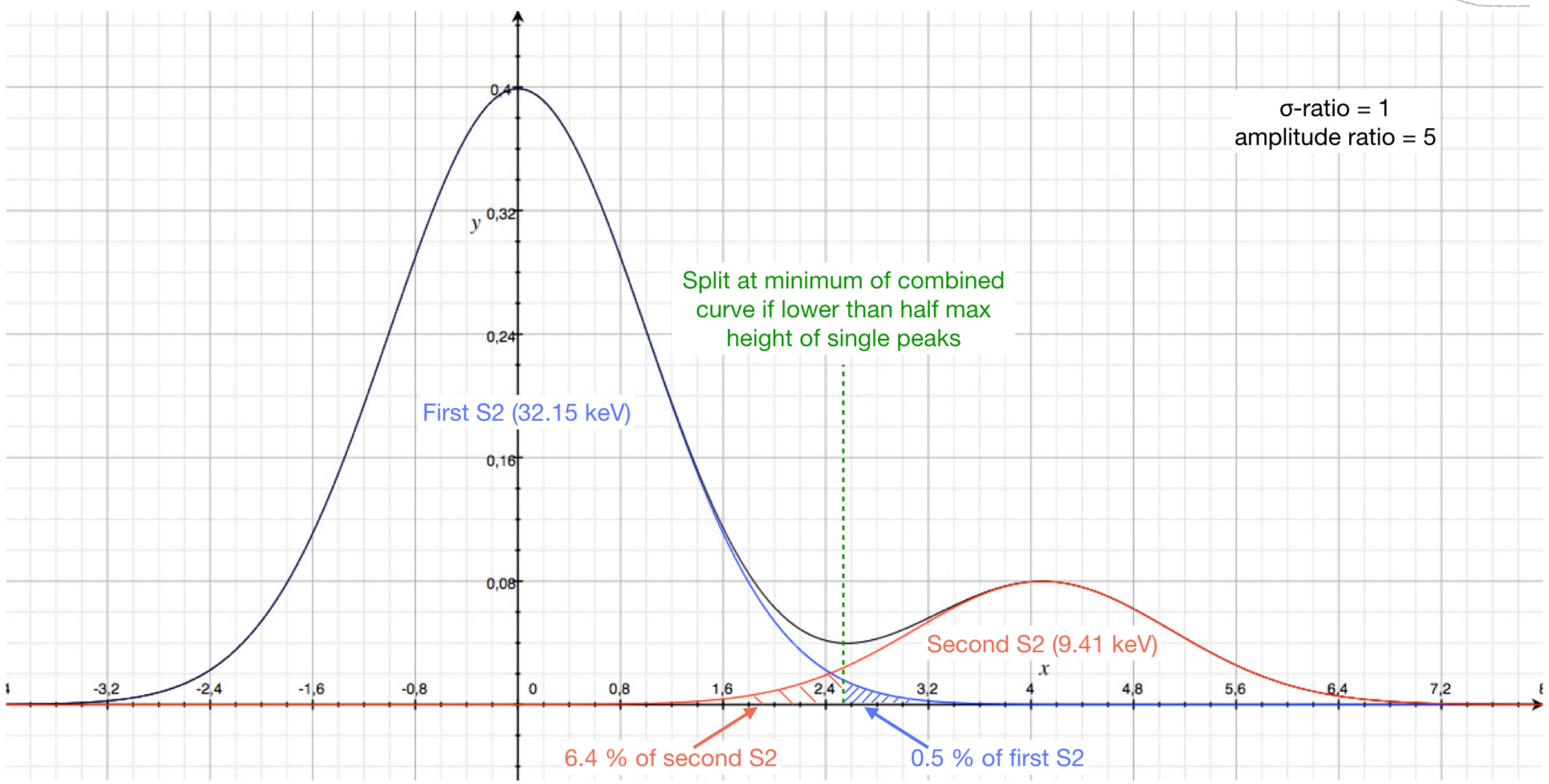

- Data-driven approach based on well-separated peaks (> 1.2 μs) -> shift together up to the point where splitting is just about possible

All of this finally yields…

W-value Result

➡ With global approach: $\boxed{\mathbf{W = 11.5^{+0.2}_{-0.3}\,(syst.)\,eV}}$

➡ Local approach yields mean values of 11.1 – 11.6 eV depending on evaluation point (energy)

- Local approach yields slightly higher uncertainties due to less direct nature of the approach
- Error dominated by systematics, and very competitive compared to former measurements
- Treated systematics from TPC, photosensor, DAQ and processing effects

- Hybrid photosensor arrangement only has limited impact
- In agreement with the EXO-200 value (@ ~keV): $\mathbf{W = (11.5 \pm 0.1\,(stat.) \pm 0.5\,(syst.))\,eV}$
- Incompatible with value from E. Dahl of $\mathbf{(13.7 \pm 0.2)\ eV}$ -> 16 % higher

Consequences

A lower W-value…

…does not affect the macroscopic energy scale (= translation from S1 & S2 signals to energy deposition) of LXe detectors -> fixed by calibration sources

…rescales the detector gains g1 & g2 of LXe detectors to lower values (-> reduced absolute response to excitation quanta)

…implies a higher Fano factor:

- Non-Poissonian fluctuation in $n := n_\gamma + n_{e^-}$: $\sigma_n = \sqrt{Fn}$
- Fano limit of energy resolution: $\frac{\sigma_E}{E} = \frac{\sigma_n}{n}$
- $\sigma_E = \sqrt{FEW}$

Universität Zürich[UZH]

PHYSIK INSTITUT
UNIVERSITÄT ZÜRICH

European Research Council
Established by the European Commission

DARWIN

Thank you for listening!

arXiv:2109.07151

darwin.physik.uzh.ch

xenoscope.org

twitter.com/darwinobserv

Backup Slides

Derivation

- Follow E. Dahl's thesis [1]:

The total number of scintillation photons is the sum of direct excitons and recombined ions,

$$N_{\mathrm{ph}} = aN_{\mathrm{ex}} + brN_{\mathrm{ion}},$$

where r is the recombination fraction and a and b are efficiencies to produce scintillation photons. For a recoil energy E, we define

$$W_q := \frac{E}{N_{\mathrm{ion}}} \qquad \text{and} \qquad W_{\mathrm{ph}} := \frac{E}{aN_{\mathrm{ex}}+bN_{\mathrm{ion}}},$$

i.e. the W-values corresponding to the total charge yield with zero recombination and the total light yield with full recombination, respectively. The number of extracted electrons is given by

$$N_q = (1-r)N_{\mathrm{ion}}.$$

Combining the equations above, we find the recombination independent sum

$$E = (N_q + \frac{N_{\mathrm{ph}}}{b})bW_{\mathrm{ph}}.$$

We identify $n_{e^-} = N_q$, $n_\gamma = N_{\mathrm{ph}}/b$ and $W = bW_{\mathrm{ph}}$. W can be interpreted as the average energy needed to produce a quantum – either an electron or a photon. The definitions yield the well-known expression

$$E = (n_{e^-} + n_\gamma)W.$$

Nuclear Recoils

$$E = \mathscr{L}^{-1}(n_\gamma + n_{e^-})W$$

Lindhard factor
(energy dependent)

- ER -> E completely converted in electronic excitation
- NR -> Elastic collisions with other nuclei (quenching)
- $N_{\mathrm{ex}}/N_{\mathrm{ion}}$ larger for NR than ER -> mean W would be lower (less energy needed for exciton than ion)

  -> However, difference can be absorbed in $\mathscr{L}$

^{37}Ar Results II

- Isolate (uncorrelated) M-shell events with time veto -> converges to right branching ratio M/L
- But branching ratio M/L increases exponentially with time -> another uncorrelated source of SE as irreducible background $BR(t) = \frac{M(t)+x_0}{L(t)} = \frac{M_0}{L_0} + \frac{x_0}{L_0} e^{\ln 2 \frac{t}{T_{1/2}}}$

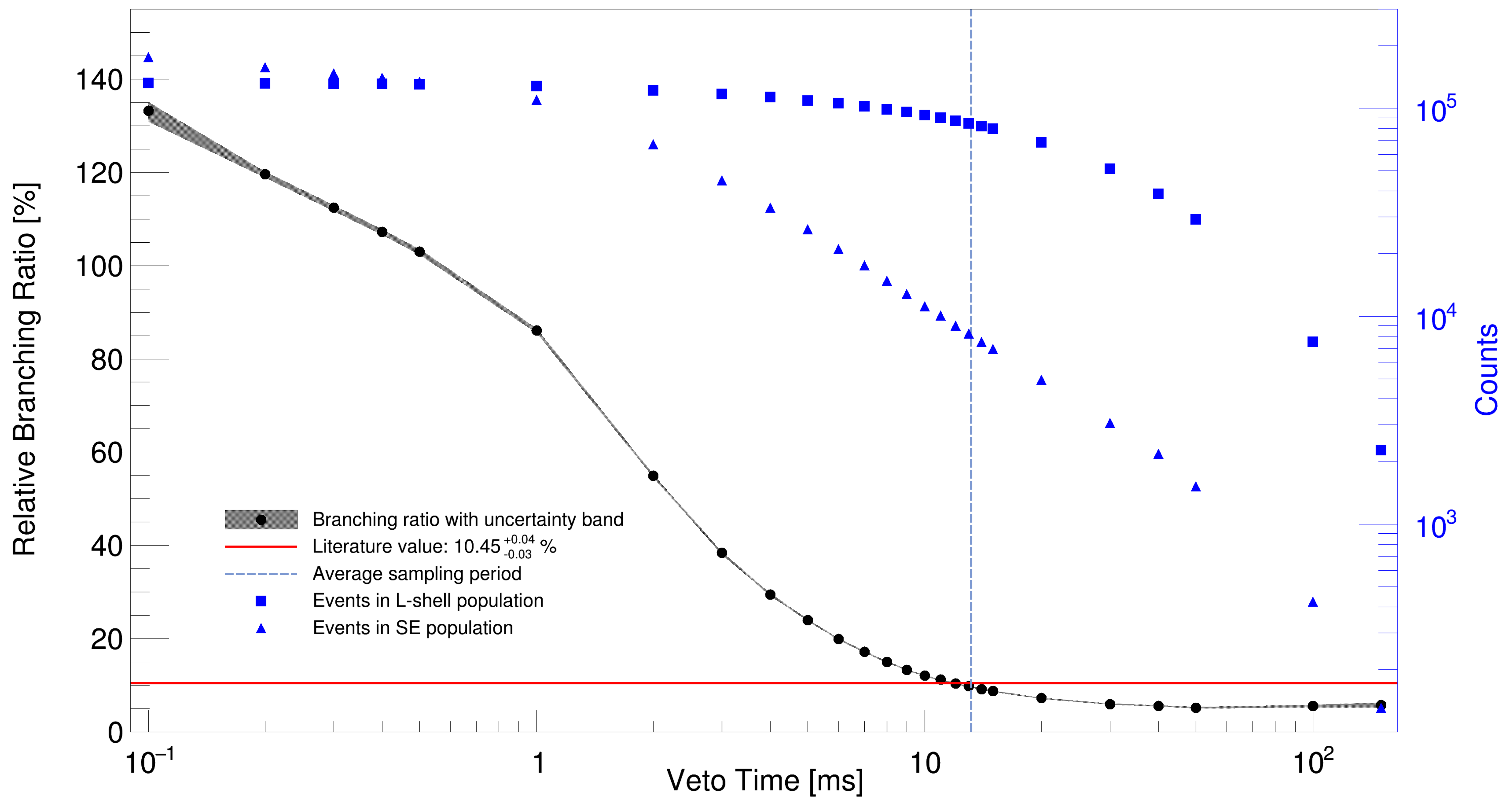

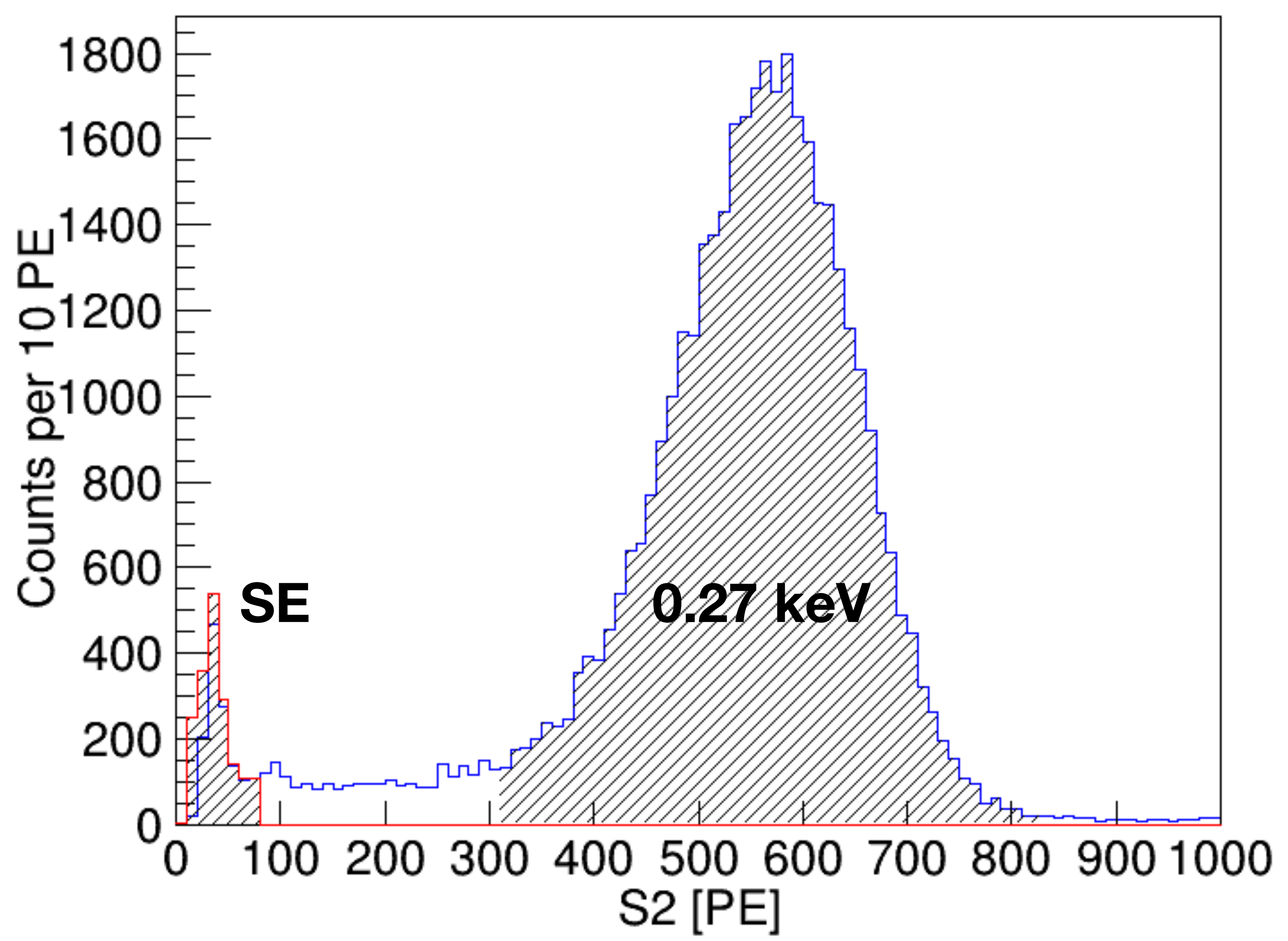

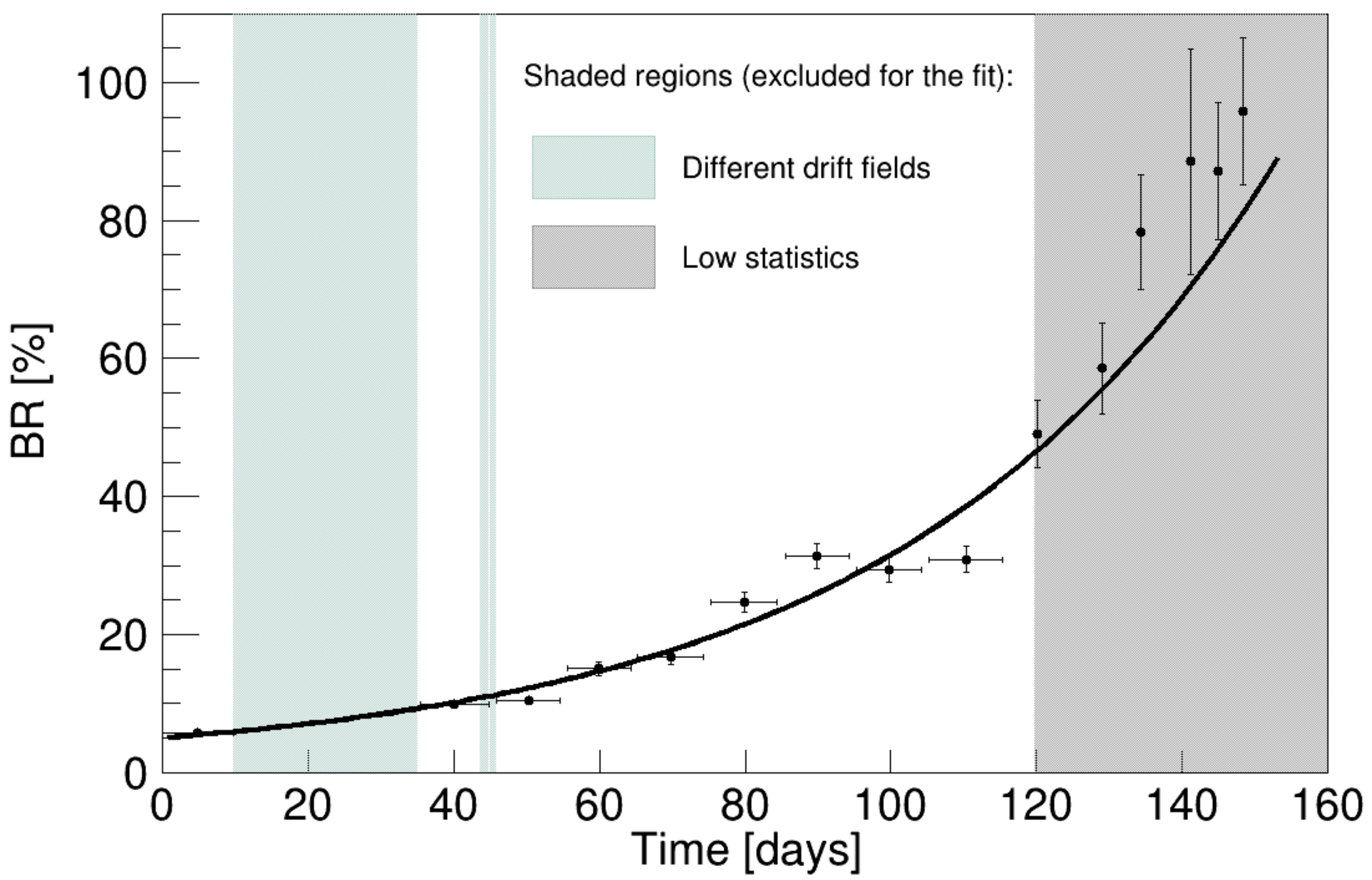

Light and Charge Yield at Low Energies

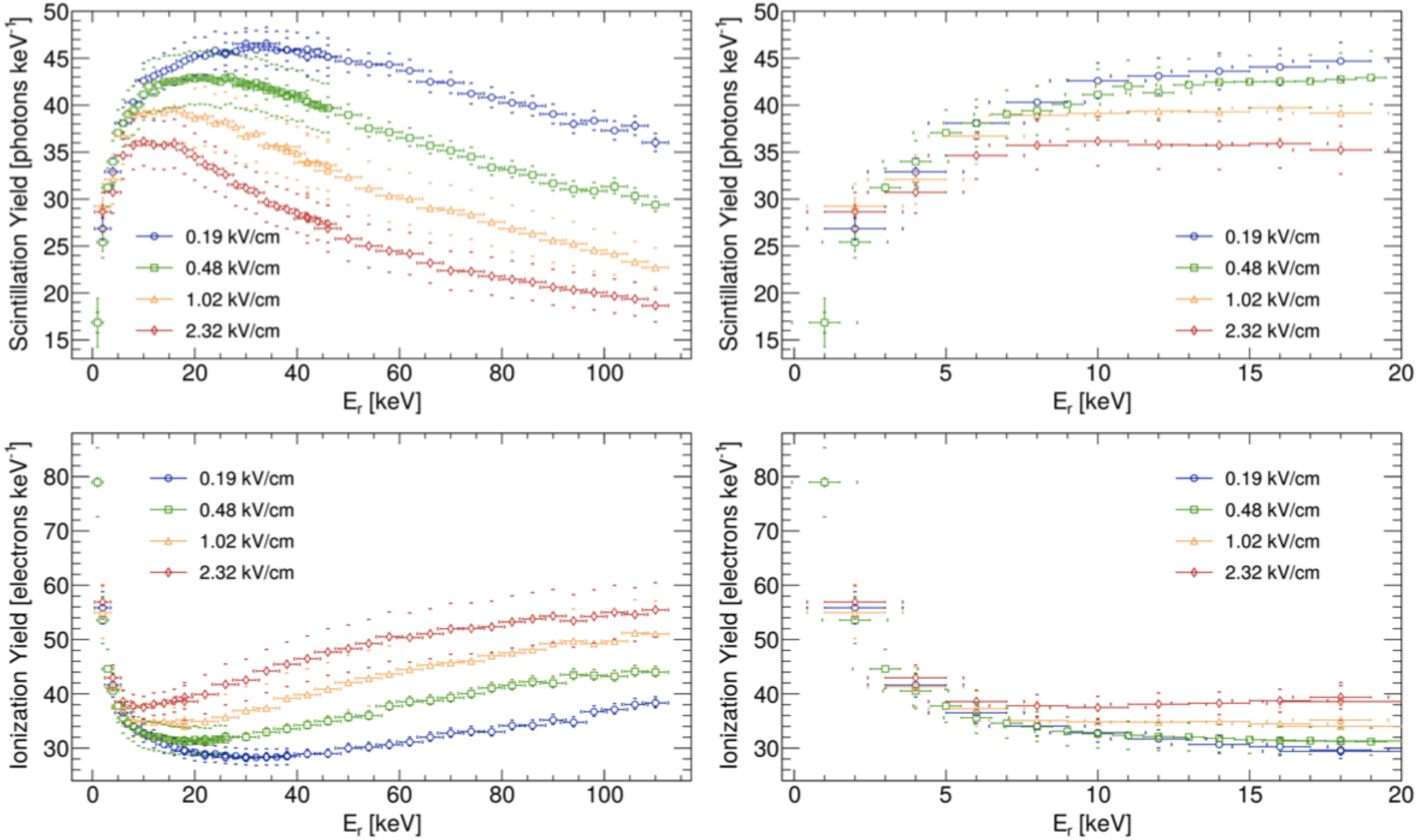

L.W. Goetzke et al., Phys. Rev. D 96, 103007 (2017)

Liquid Xenon Purity and TPC Geometry

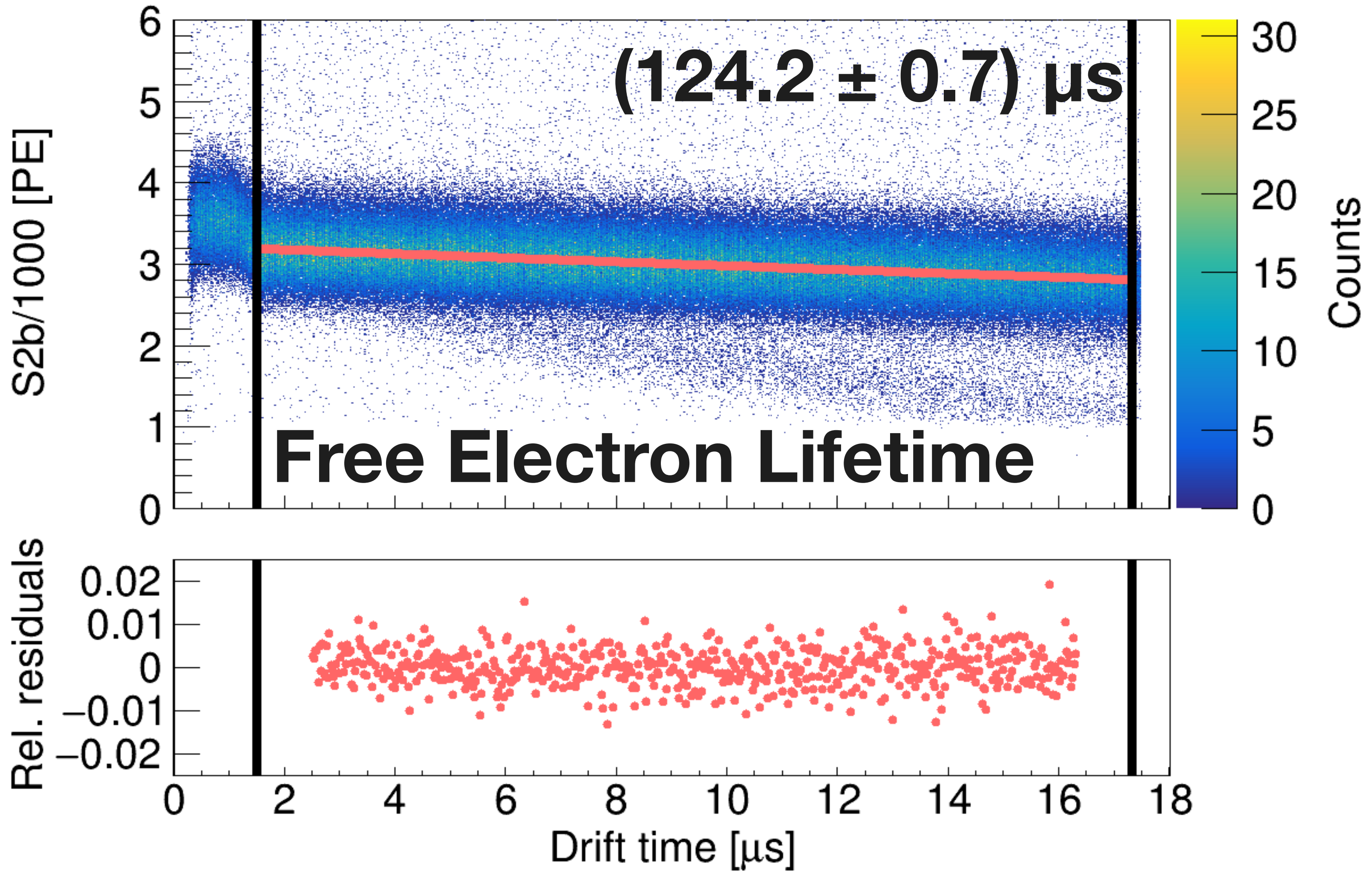

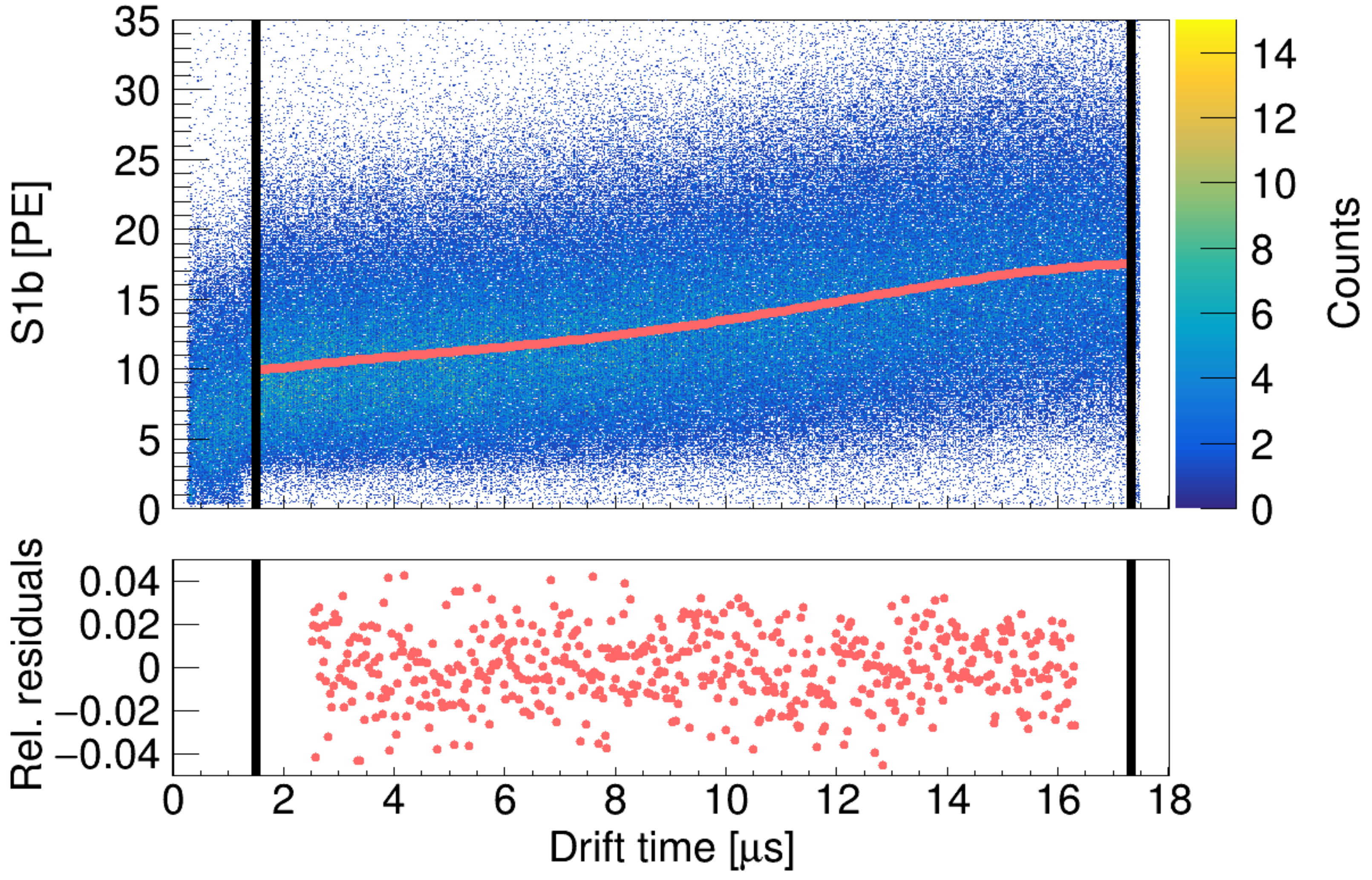

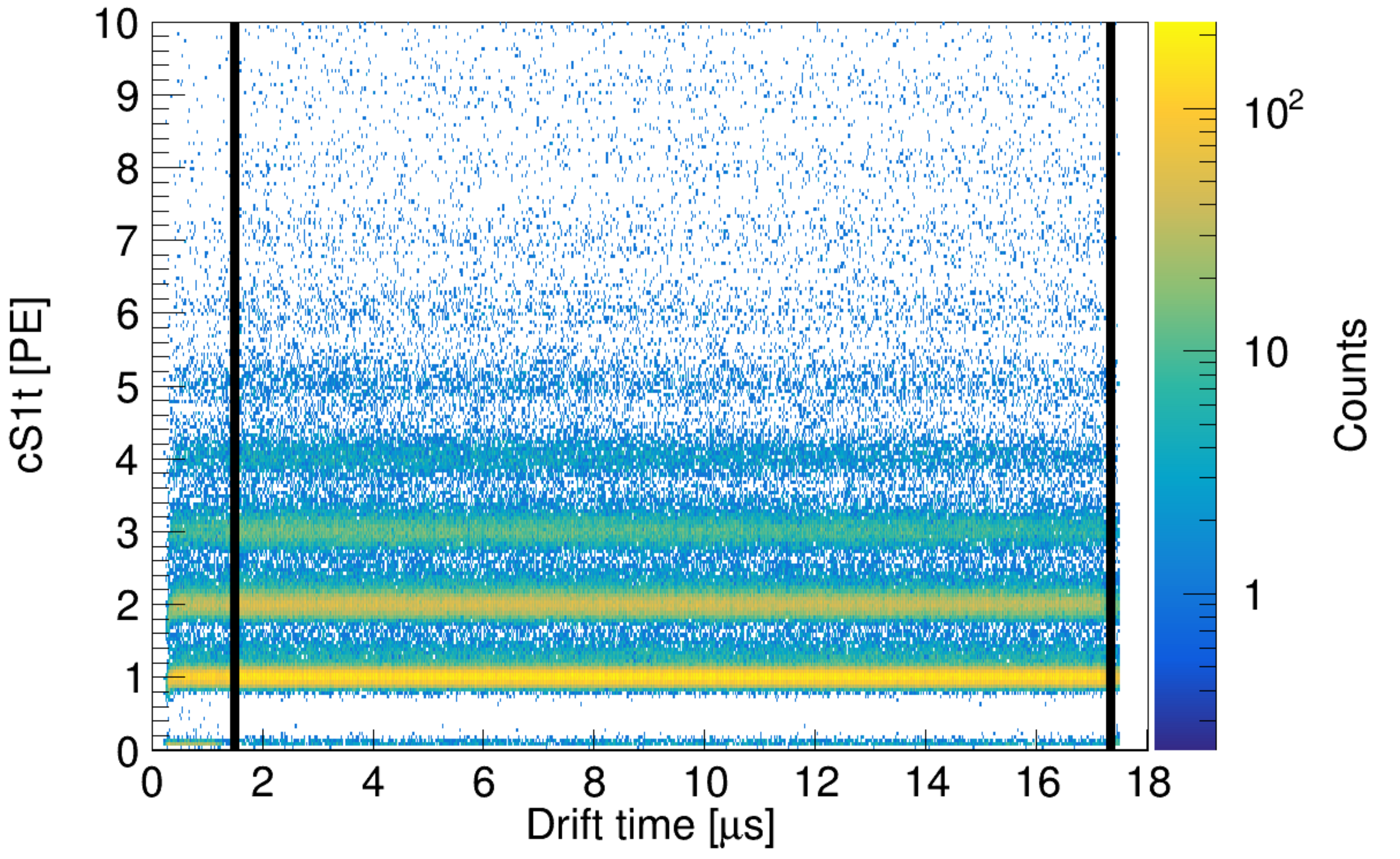

- Data is fiducialised and drift time related systematics in S1 and S2 are corrected

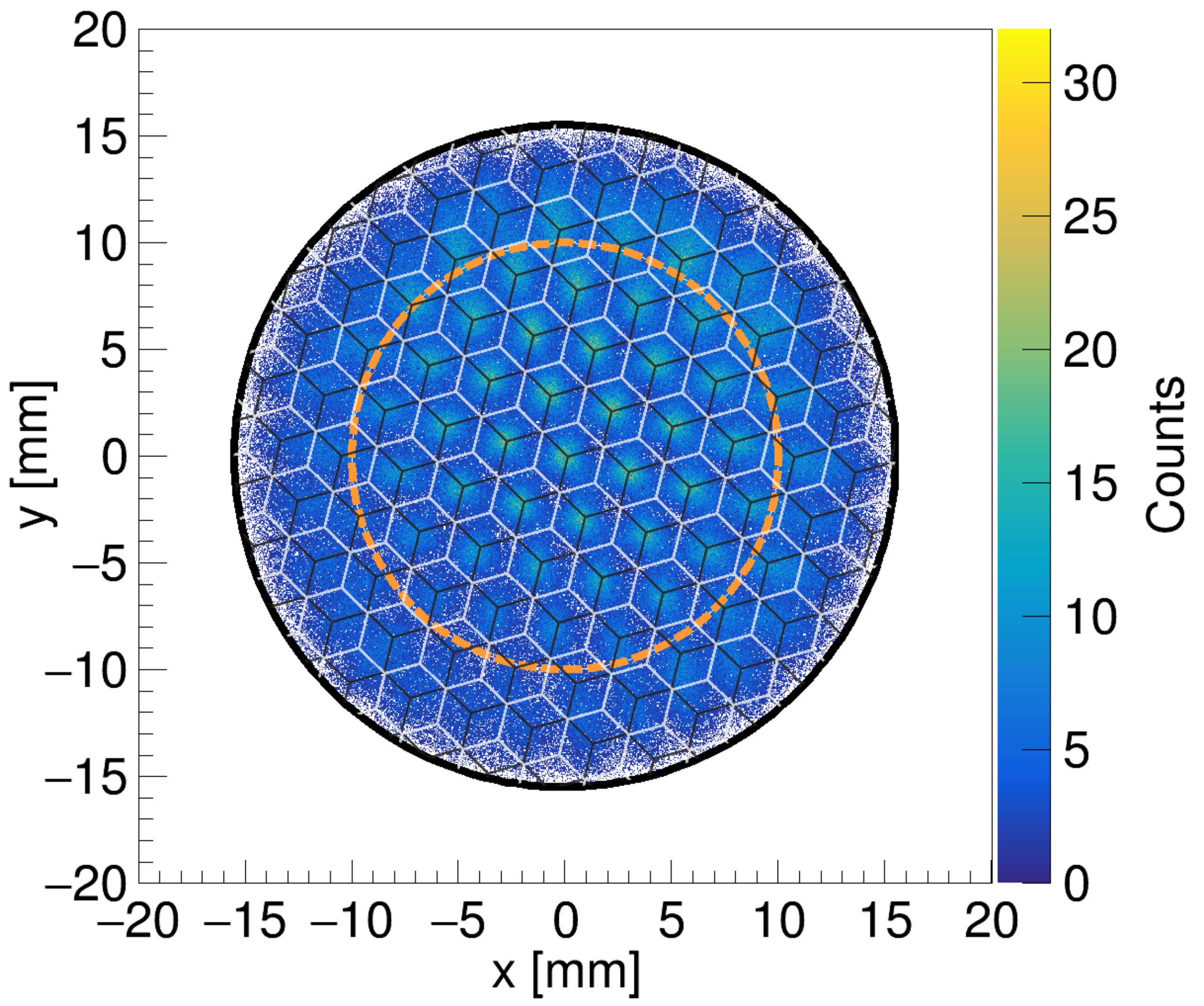

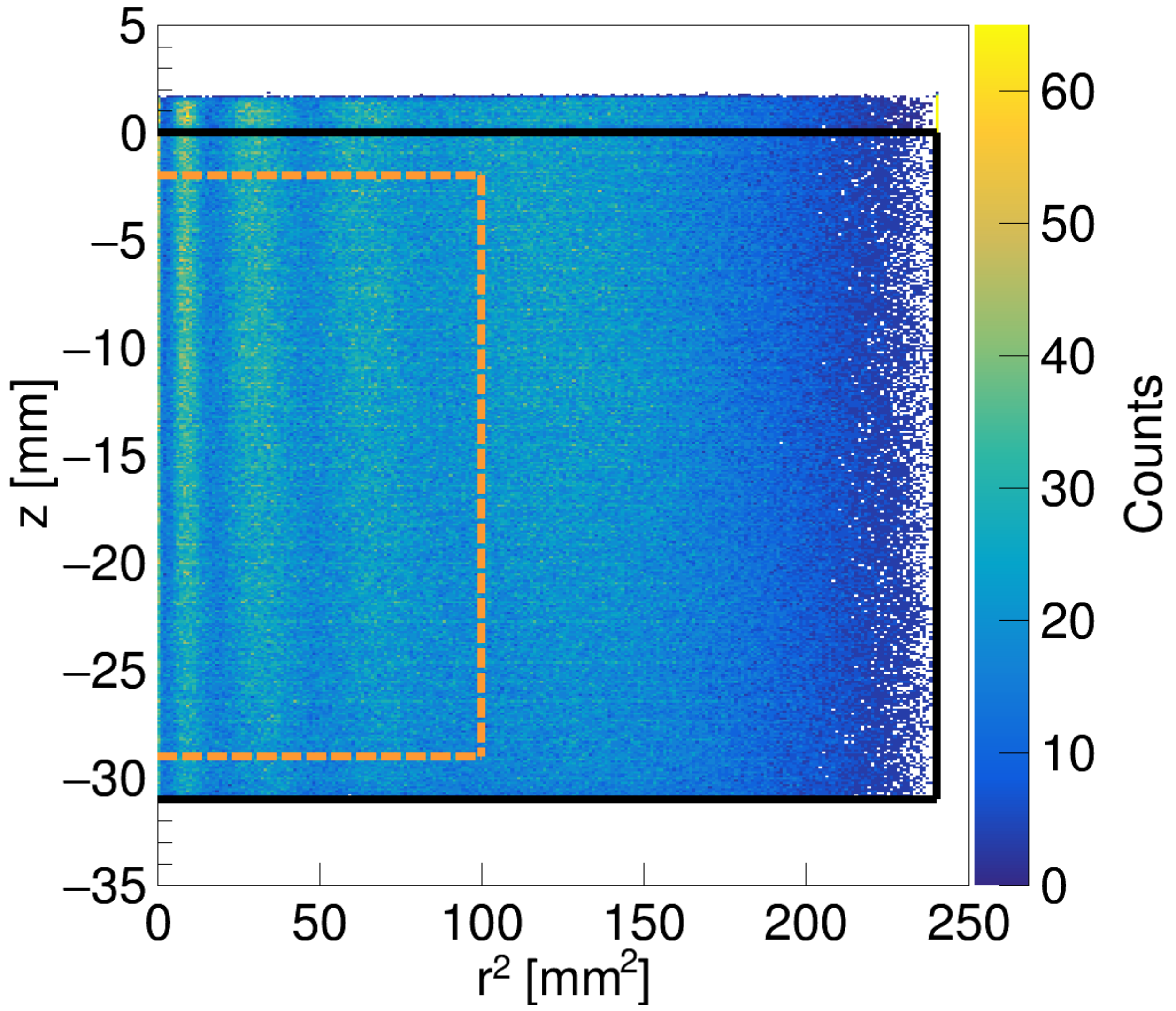

- Assume pressure, density and purity fluctuations, and attenuation length beyond the corrections to be negligible

EPJ C 80, 477 (2020)

S2-Gain – Liquid Level

- Assumed constant at 2 mm during the runs (4 mm between gate and anode)
  - Temperature range liquid: 0.4 K
  - Pressure range: 0.05 bar
  - Recirculation rate range: 0.1 slpm
- Leveling procedure gives rise to 125 µm change in liquid level among runs <-> 2.5 % in S2 (one major devision of motion feedthrough)
- Tilting in x-y covered by this uncertainty
- S2 change from linear interpolation between 1.5 mm and 2.125 mm

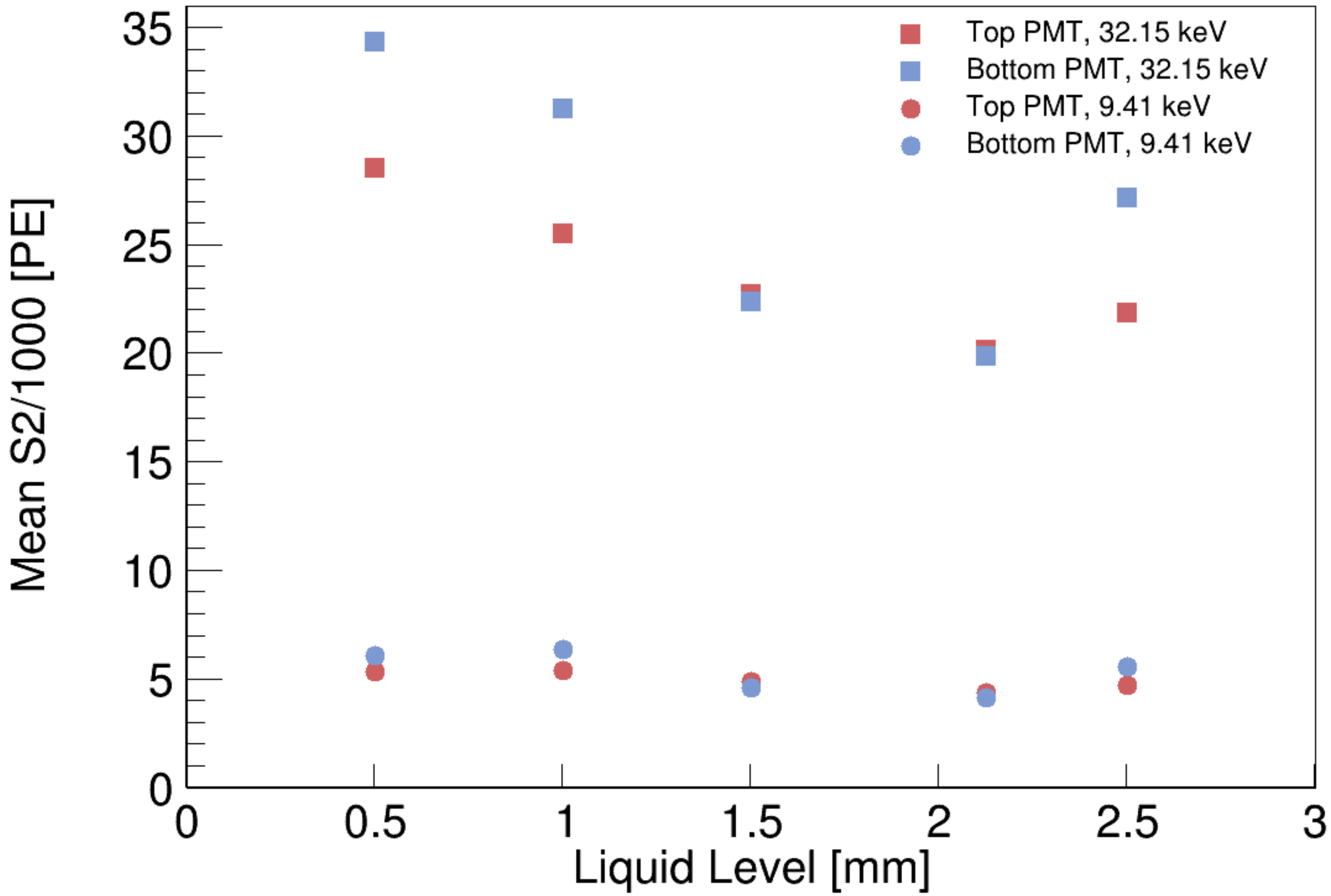

Electron Extraction Efficiency

- Extraction efficiency at 10 kV/cm (5.4 kV/cm in LXe) is assumed to be 100 % [4,5]
- W-value would only be lower for lower efficiencies

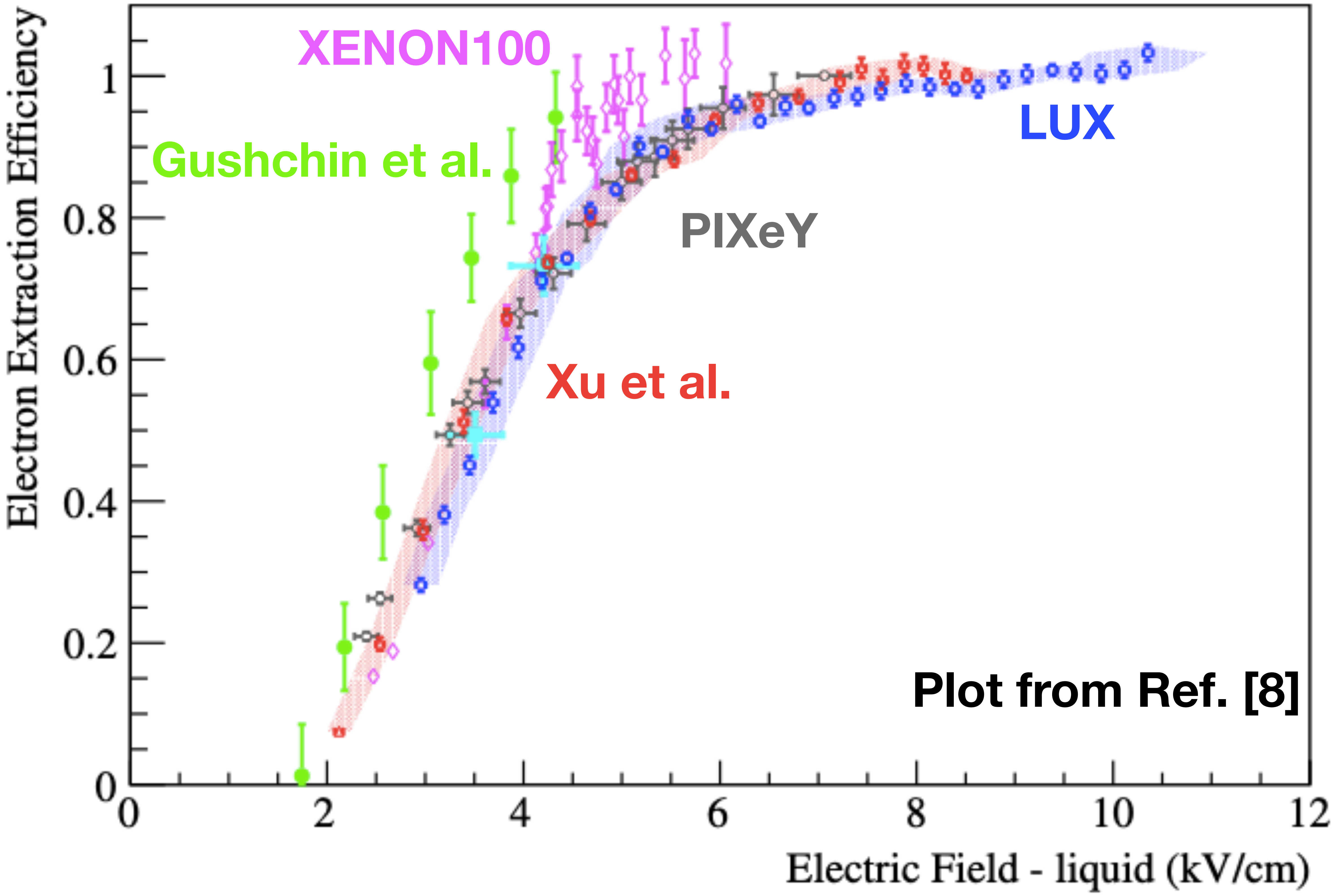

[7] B. N. V. Edwards et al. JINST 13, no. 1, P01005 (2018)

[8] J. Xu et al., Phys. Rev. D 99, no. 10, 103024 (2019)

Photosensor Effects

Hybrid Photosensor Configuration

- ➡ Rewrite W for three points a, b, c in S1-S2 space and express top by bottom contributions (γs for S2s and $\bar{\gamma}$s for S1s):

$$W = E \cdot \frac{\phi \cdot \mathrm{S2b}_c \cdot (\eta_{\mathrm{PMT}} + \eta_{\mathrm{SiPM}}\gamma_c)}{\frac{\phi \cdot \frac{\mathrm{S2b}_a}{E_a}(\eta_{\mathrm{PMT}} + \eta_{\mathrm{SiPM}}\gamma_a) - \phi \cdot \frac{\mathrm{S2b}_b}{E_b}(\eta_{\mathrm{PMT}} + \eta_{\mathrm{SiPM}}\gamma_b)}{\phi \cdot \frac{\mathrm{S1b}_b}{E_b}(\eta_{\mathrm{PMT}} + \eta_{\mathrm{SiPM}}\tilde{\gamma}_b) - \phi \cdot \frac{\mathrm{S1b}_a}{E_a}(\eta_{\mathrm{PMT}} + \eta_{\mathrm{SiPM}}\tilde{\gamma}_a)} \cdot \phi \cdot \mathrm{S1b} \cdot (\eta_{\mathrm{PMT}} + \eta_{\mathrm{SiPM}}\tilde{\gamma}) + \phi \cdot \mathrm{S2b} \cdot (\eta_{\mathrm{PMT}} + \eta_{\mathrm{SiPM}}\gamma)}$$

- ➡ γ and $\bar{\gamma}$ depend on geometry, reflections, … that influence the top/bottom light collection
- ➡ ηs are photosensor efficiencies and expected to be energy and time independent for unchanged thermodynamical conditions
- ➡ W is insensitive to overall time-constant, and energy- and sensor-independent factor ϕ in g1, g2, S1, S2 like ADC-to-PE
- ➡ But $\gamma \neq \gamma_a \neq \gamma_b \neq \gamma_c$ (same for ¯) -> ηs do have an impact!

Energy [keV]	Light yield fraction [%] Top SiPMs / Bottom PMT	Charge yield fraction [%] Top SiPMs / Bottom PMT
se	— / —	18—19 / 81—82
2.82	10—11 / 89—90	25—27 / 73—75
9.41	7 / 93	20—21 / 79—80
32.15	7—8 / 92—93	31—32 / 68—69
41.56	7—8 / 92—93	29—30 / 70—71

From low-discrete PE in the top

From Splitting

Photosensor Effects

Photosensor Gain

- PMT: (3.76 ± 0.06) × 10⁶
- SiPM: (3.12 ± 0.01) × 10⁶
- 1σ assumed as variation in time

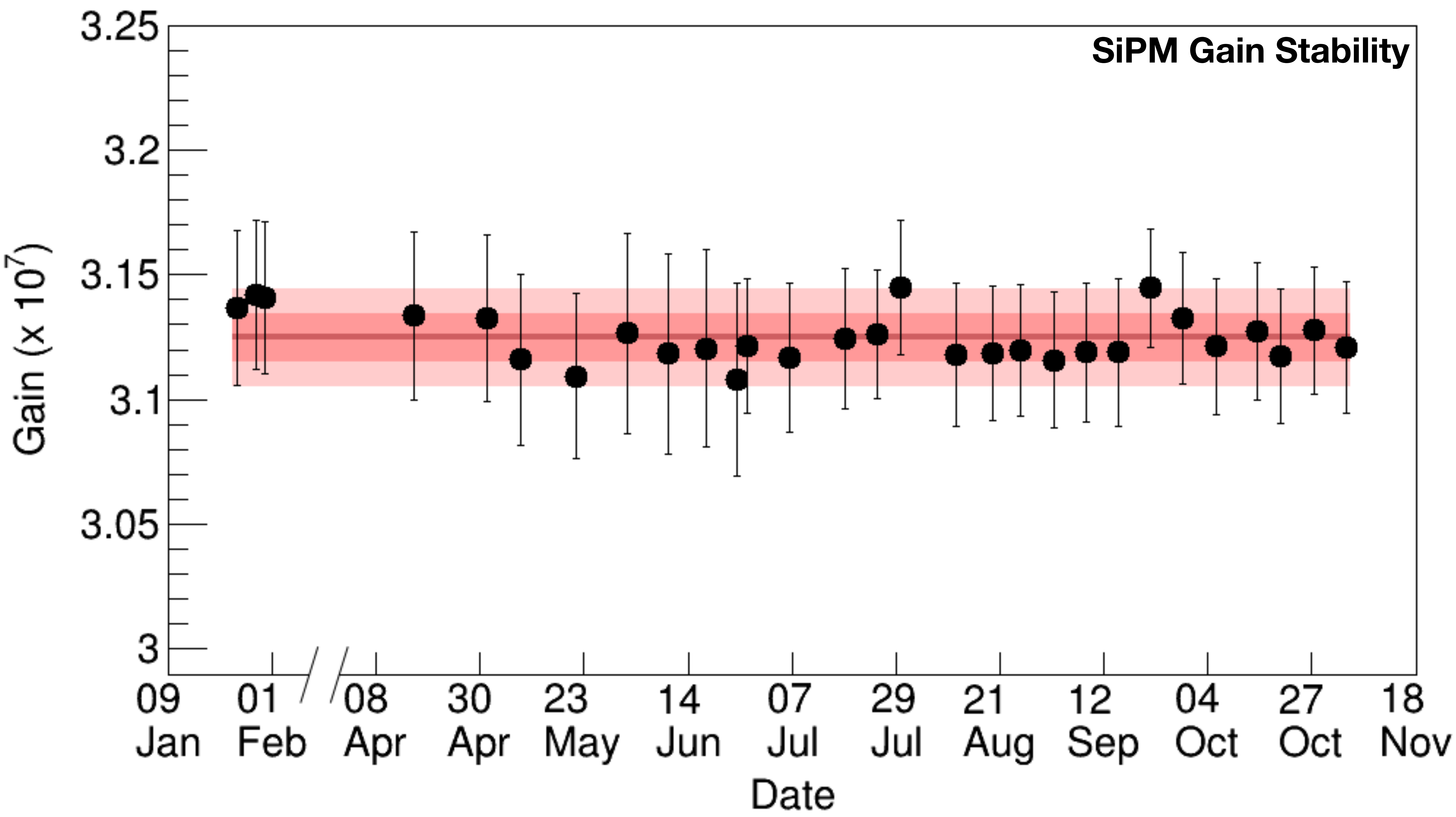

Photon Detection Efficiency

- VUV-4 SiPM:
  - PDE = 24 % (Hamamatsu Photonics)
  - PDE = 9.9–17.6 % at 3.3–3.8 V OV (nEXO [9–10]) -> we have > 4 V OV
- 2-inch PMT:
  - QE = 30 % (Hamamatsu Photonics)
  - QE = 28 % [11]
  - CE = ~70 % (Hamamatsu Photonics)
  - -> PDE = 19.6–21 %
- Very similar, max. percent-level difference

@175–178 nm

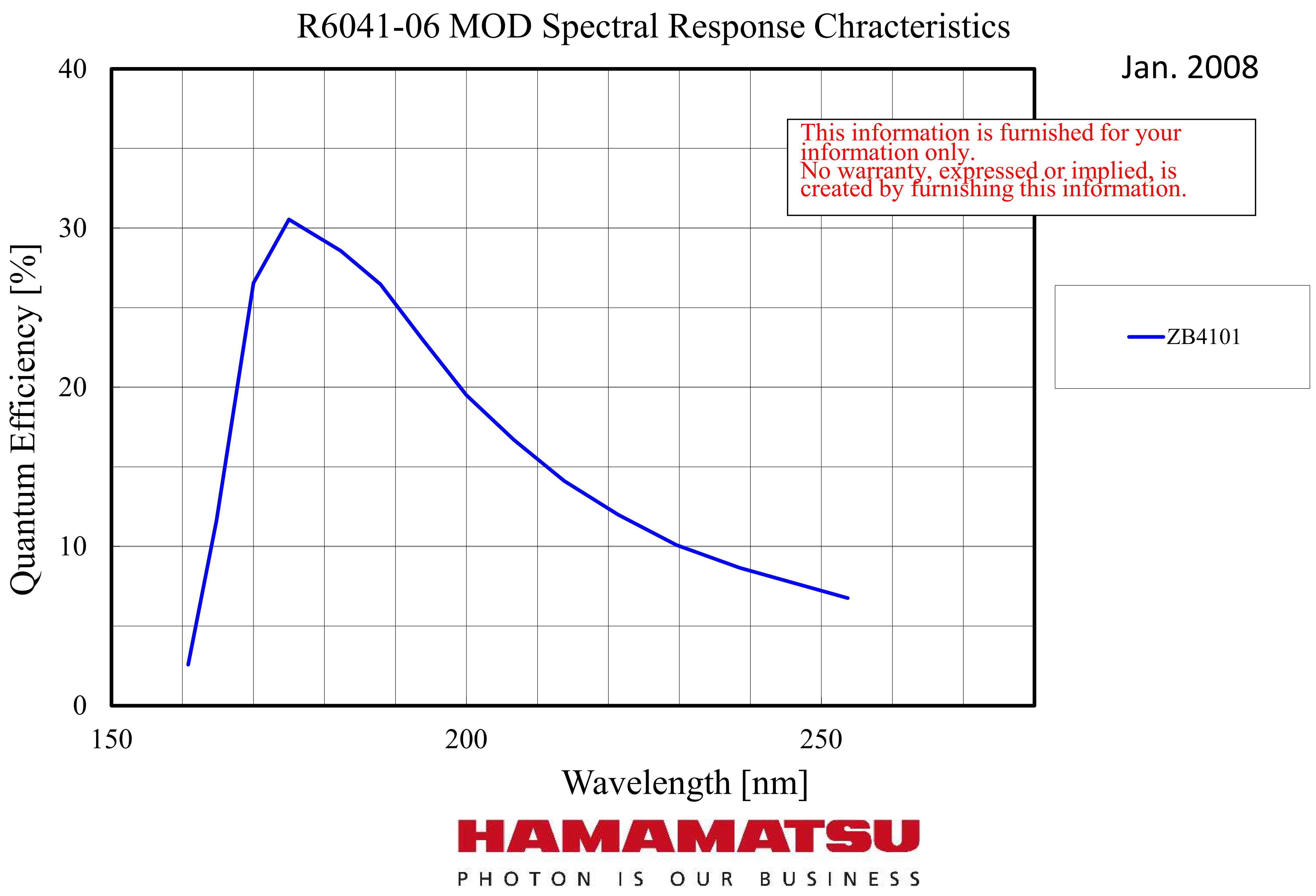

[9] G. Galina et al., Nucl. Instrum. Meth. A 940, 371–379 (2019)
[10] P. Nakarmi et al., JINST 15 P01019 (2020)
[11] L. Arazi et al., JINST 8 C12004 (2013)

Infrared Sensitivity

- GXe scintillates in the IR at ~1300 nm with VUV-comparible yield [13–14]
- LXe IR very poor light yield mostly below 1200 nm [12–13]
- -> Only S2 can contain significant IR radiation
- VUV-4 SiPM:
    - Silicon band gap sets cutoff at ~1100 nm
- 2-inch PMT:
    - Insensitive beyond 1000 nm
- -> IR radiation negligible

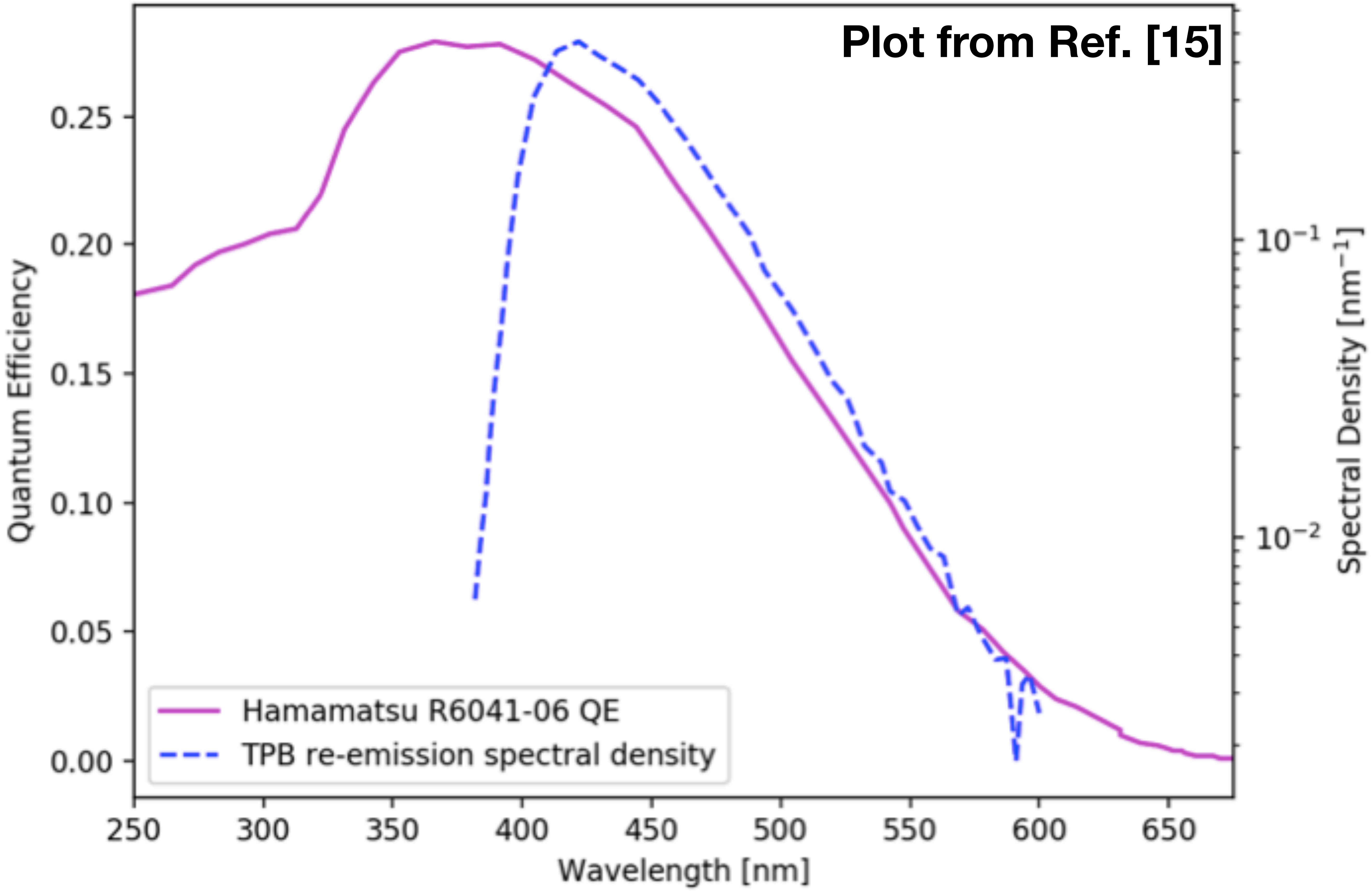

[12] G. Bressi et al., Nucl. Instrum. Methods Phys. Res A 440 254–257 (2000)
[13] G. Bressi et al., Nucl. Instrum. Methods Phys. Res A 461 378–380 (2001)
[14] S.Belogurov et al., Nucl. Instrum. Methods Phys. Res A 452 167–169 (2000)
[15] J. Schrott et al., arXiv:2108.08239 (2021)

DAQ/Processing Effects

Fitting Errors

- Systematic variation of fitting interval for 2.82 keV population

➡ $\Delta S1 =^{+0.1}_{-0.6}$ PE

➡ $\Delta S2 =^{+8}_{-30}$ PE

(not DPE/crosstalk-scaled)

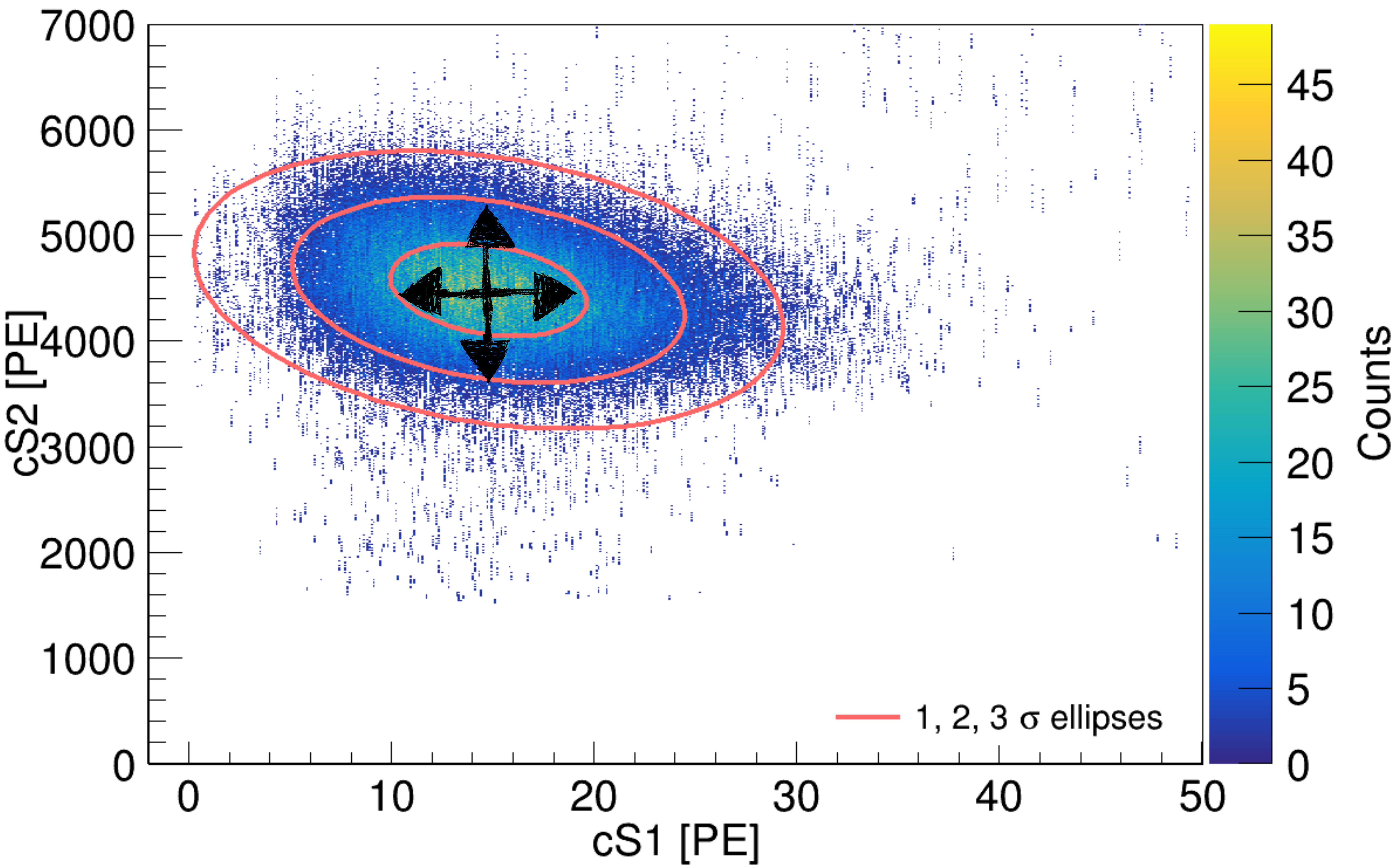

Bottom-PMT Only

- Check consistency using PMT-only information
- Doke-plot is shallower due to greater S1- and lower S2-yield in the liquid
- Splitting error is more pronounced -> use 41.56 keV line (but does not change slope anyways)
- Why's that? -> AFT cut incorporated for Ar- & Kr-lines!
- SE population has very low AFT-fractions (single photon regime) -> higher PMT charge yield
- AFT cut has bad acceptance for SE
- Can generate any PMT-based g2 & W by applying different AFT cuts to SE but total g2 & W always stay constant!